UNIVERSITA' POLITECNICA DELLE MARCHE

FACOLTA' DI INGEGNERIA

Corso di Laurea triennale in Ingegneria Gestionale

Analisi delle proprietà termodinamiche dell'idrogeno e dell'idrogeno in miscele

Analysis of thermodynamic properties of H2 and H2-rich mixtures

Relatore:

Prof. Francesco Corvaro

Tesi di laurea di:

Sara Tatani

Matr.1089955

Correlatore:

Ing. Matteo Vitali

A.A. 2020 / 2021

Abstract

What is reported below is intended to inform the reader of some things, in particular the thermodynamic properties of hydrogen and hydrogen in mixtures. Five experiments will be analyzed in all their aspects, namely the methods used to carry them out, the details, the procedures, the tools and above all the equations of state used both for hydrogen and its mixtures. The analyzed experiments were taken from various English scientific journals. The methods describe the various procedures carried out in the five experiments and how they are carried out. The instruments used and the sizes are shown in the details. The equations of state describe the models for both hydrogen and hydrogen in mixtures. Specifically, all the models are listed through the equations that lead to the resolution of the various experiments, such as the GERG-2008 and AGA8-DC92, the Peng-Robinson. Furthermore, we can also note the various changes in state of hydrogen, where it can be found and how it can be obtained.

Riassunto dell’elaborato in lingua italiana

La presente tesi è volta a descrivere le proprietà termodinamiche dell’idrogeno e dell’idrogeno in miscele attraverso l’analisi di alcuni esperimenti tratte dalle più importanti riviste scientifiche inglesi. Questa analisi viene fatta attraverso delle equazioni di stato che ci spiegano come l’idrogeno può cambiare in tutte le sue forme anche miscelato. Nel primo esperimento l'equazione di stato GERG-2008 è lo standard ISO approvato per il calcolo delle proprietà termofisiche di miscele di gas naturale. La composizione del gas naturale può variare notevolmente a causa della diversità e della provenienza. Un'ulteriore diversificazione è stata generata aggiungendo idrogeno, biogas o altri gas energetici non convenzionali. In questo esperimento, sono riportati dati sperimentali ad alta precisione (p, r, T) per undici miscele di gas naturale. Nel secondo esperimento vediamo che l'uso dell'idrogeno (H2) rappresenta la maggior parte dei consumi mondiali. In questo studio è stata utilizzata l'equazione GERG-2008 e il modello SupertRaPP per prevedere le proprietà termofisiche dell’idrogeno miscelato con il metano, l’azoto e l’anidrite carbonica ed un tipico gas del Mare del Nord. Nel terzo esperimento undici equazioni di stato sono impiegate per prevedere le pressioni di vapore, liquido e vapore, densità, capacità di calore del liquido e del vapore, entalpie ed entropie di vaporizzazione dell’idrogeno normale lungo la curva di coesistenza. I risultati vengono confrontati con i dati sperimentali e i valori raccomandati dalle tavole termodinamiche. Vengono riportate e introdotte le migliori equazioni di stato per predire le proprietà dell'idrogeno. Nel quarto esperimento si evince il comportamento termodinamico dell’idrogeno miscelato con il metano attraverso queste equazioni di stato: Benedict-WebbRubin (BW R), Soave-Redlich-Kwang e PengRobinson. I dati raccolti per questa miscela si trovano nell’intervallo da 100°F a -200°F e sono contenute all’interno anche le componenti polari come l’idrogeno solforato e l’anidrite carbonica. Infine, nell’ultimo esperimento ovvero nel quinto si evince un’indagine sulle proprietà termodinamiche dell’idrogeno normale e del paraidrogeno e vengono forniti confronti di proprietà calcolate dai

modelli standard ai dati sperimentali disponibili. Lo stato attuale delle equazioni di stato per l'idrogeno normale e il paraidrogeno stabilisce le priorità per lo sviluppo di nuovi modelli estendendo le gamme di temperatura e pressione.

Contents

1 INTRODUCTION

Hydrogen is the first chemical element on the periodic table (atomic number 1) and the lightest. In the free state, at atmospheric pressure and room temperature (298 K), it is found in the form of diatomic gas having the formula H2, colorless, odorless, tasteless and highly flammable, with a boiling point of 20.27 K and a melting point 14.02 K. In the bound state it is present in water (11.19%) and in all organic compounds and living organisms; moreover, it is occluded in some rocks, such as granite, and forms compounds with most of the elements, often also by direct synthesis. It is the main constituent of stars, where it is present in the plasma state and represents the fuel of thermonuclear reactions, while on Earth it is scarcely present in the free and molecular state and must therefore be produced for its various uses. Hydrogen combines with most of the elements. Through some equations of state, the thermodynamic properties of both hydrogen and its mixtures are deduced. The purpose of this work is to draw up a state of the art through a bibliographic search in the most important scientific journals. Specifically, experiments carried out by different scientists are analyzed and a series of data are compared. Through a series of state equations relating to both hydrogen and its mixtures, the related thermodynamic properties that characterize them are defined. Finally, conclusions will be drawn trying to exploit all the results obtained from these experiments.

Abbreviations

NIST	National Institute of Standard
PR	Peng-Robinson
EoS	Equation of State
SRK	Soave-Redlich-Kwong
AAD	Average Absolute Deviation
NB	Nasrifar–Bolland
PRGGPR	Peng–Robinson–Gasem–Gao–Pan–Robinson
PRMC	Peng–Robinson–Mathias–Copeman
PRSV	Peng–Robinson–Stryjek–Vera
PRTCC	Peng–Robinson–Twu–Coon–Cunningham
PSRK	Predictive Soave–Redlich–Kwong
PT	Patel–Teja
PTV	Patel–Teja–Valderrama
RK	Redlich–Kwong
RKS	Redlich–Kwong–Soave
RKMC	Redlich–Kwong–Mathias–Copeman
RKSW	Redlich– Kwong–Square-Well
SAFT-VR	Statistical associating fluid theory with variable range

2 EXPERIMENTAL DATA

In this chapter, experimental data collected during the literature review are reported. A total of 5 experiments have been analyzed in this work. In Table 1, a summary of the experiments most relevant details including the experiment title, the authors and their affiliations have been included.

	Experiment title	Authors	Affiliations
1	Accurate experimental (p, r, T) data of natural gas mixtures for the assessment of reference equations of state when dealing with hydrogen-enriched natural gas	Roberto Hernandez [a], Gomez, Dirk Tuma [b], Daniel Lozano-Martin [a], Cesar R. Chamorro [a]	[a] Grupo de Termodinamica y Calibracion (TERMOCAL), Dpto. Ingenierìa Energética y Fluidomecanica Escuela de Ingenierìas Industrìales, Universidad de Valladolid, Paseo del Cauce, 59, E-47011 Valladolid, Spain [b] BAM Bundesanstalt für Materialforschung und -prüfung, D-12200 Berlin, Germany
2	Thermodynamic and transport properties of hydrogen containing streams	Aliakbar Hassanpouryouzband [1], Edris Joonaki[2], Katriona Edlmann[1], Niklas Heinemann[1] & JinhaiYang[3]	[1] School of Geosciences, University of Edinburgh, Grant Institute, West Main Road, Edinburgh, EH9 3JW, UK [2] TÜV SÜD National Engineering Laboratory, Scottish Enterprise Technology Park, East Kilbride, South Lanarkshire, G75 0QF, United Kingdom. [3] Hydrates, Flow Assurance & Phase Equilibria Research Group, Institute of GeoEnergy Engineering, School of Energy,

			Geoscience, Infrastructure and Society, Heriot-Watt University, Riccarton, Edinburgh, EH14 4AS, UK.
3	Comparative study of eleven equations of state in predicting the thermodynamic properties of hydrogen	Khashayar Nasrifar	Department of Chemical Engineering, Shiraz University of Technology, Modares Blvd., Shiraz, Iran
4	Thermodynamic behavior of hydrogen/natural gas mixtures	R. R. Agahi, B. Ershaghi, M. C. Lin and G. A. Mansoori(*)	University of Illinois at Chicago
5	Current Status of Thermodynamic Properties of Hydrogen	R. T Jacobsen [1] · J. W. Leachman [2] · S. G. Penoncello [2]· E. W. Lemmon [3]	[1] College of Engineering, Idaho State University, Pocatello, ID, 83209-8060 [2] Center for Applied Thermodynamic Studies (CATS), University of Idaho, Idaho Falls, Moscow, ID 84844, USA [3] Physical and Chemical Properties Division, National Institute of Standards and Technology, Boulder,CO 80305-3328, USA

Table 1 – Summary of experimental data analysed

In the first experiment, the GERG-2008 equation of state was approved by ISO to proceed with the calculation of the thermophysical properties of gas mixtures. The composition of natural gas can vary considerably due to the diversity of origin. Further diversification was generated by adding hydrogen, biogas, or other non-conventional energy gases. High-precision experimental (p, r, T) data

for two gravimetrically prepared synthetic natural gas mixtures are reported. One mixture resembled a conventional natural gas of 11 components with a nominal mixture composition (amount-of-substance fraction) of 0.8845 for methane as the matrix compound with the other compounds being 0.005 for oxygen, 0.04 for nitrogen, 0.015 for carbon dioxide, 0.04 for ethane, 0.01 for propane, 0.002 each for n- and isobutane, and ultimately 0.0005 each for isopentane, n-pentane, and n-hexane. The other mixture was a 13-component hydrogen-enriched natural gas with a low calorific value featuring a nominal composition of 0.7885 for methane, 0.03 for hydrogen, 0.005 for helium, 0.12 for nitrogen, 0.04 for carbon dioxide, 0.0075 for ethane, 0.003 for propane, 0.002 each for n- and isobutane, and 0.0005 each for neopentane, isopentane, n-pentane, and n-hexane. Density measurements were performed in an isothermal operational mode at temperatures between 260 and 350 K and at pressures up to 20 MPa by using a single sinker densimeter with magnetic suspension coupling. The data were compared with the corresponding densities calculated from both GERG-2008 and AGA8-DC92 equations of state to test their performance on real mixtures. The average absolute deviation from GERG-2008 (AGA8-DC92) is 0.027% (0.078%) for 11 components and 0.095% (0.062%) for the 13- component H2-enriched mixture, respectively. The corresponding maximum relative deviation from GERG-2008 (AGA8-DC92) amounts to 0.095% (0.127%) for 11 components and 0.291% (0.193%) for the H2-rich mixture. In the second experiment according Aliakbar Hassanpouryouzband, Edris Joonaki, Katriona Edlmann, Niklas Heinemann and JinhaiYang the use of hydrogen (H2) as a substitute for fossil fuel, which accounts for most of the the world's energy, is environmentally the most benign option for the reduction of CO2 emissions. This will require gigawatt-scale storage systems and as such, H2 storage in porous rocks in the subsurface will be required. Accurate estimation of the thermodynamic and transport properties of H2 mixed with other gases found within the storage system is therefore essential for the efficient design for the processes involved in this system chain. In this study, they used the established and regarded GERG-2008 Equation of State (EoS) and SuperTRAPP model to predict the thermo-physical properties of H2 mixed with CH4, N2, CO2, and a typical natural gas from the North-Sea. The data covers a wide range of mole fraction of H2 (10–90 Mole%), pressures (0.01–100MPa), and temperatures (200–500K) with high accuracy and precision. Moreover, to increase ease of access to the data, a user-friendly software (H2Themobank) is developed and made publicly available. In the third experiment of Khashayar Nasrifar of the Department of Chemical Engineering, Shiraz University of Technology, Modares Blvd., Shiraz, Iran, eleven equations of state are employed to predict the vapor pressures, liquid and vapor densities, liquid and vapor heat capacities, and vaporization enthalpies and entropies of normal hydrogen

along the coexistence curve. Most of these mathematical models are for single phase gas mixtures with high pressures and warmer than cryogenic temperatures. Process plants such as ethylene plants, Methyl Tertiary Butyl Ether (MTBE) plants, and hydrogen purification plants operate at medium pressures, with cryogenic temperature, and in the two-phase region. An accurate vapor-liquid equilibrium condition for the hydrogen rich mixture is an essential prerequisite in the design of their process plants handling such mixtures. The authors evaluate the available mathematical models for the equations of state of hydrogen mixtures. Evaluation is carried out using field performance data from several plants. The fifth test presents a survey of the thermodynamic properties of normal hydrogen and parahydrogen (molecular form of hydrogen, in which the spins of the 2 protons making up the nuclei of the 2 atoms that make up the molecule are antiparallel) and gives comparisons of properties calculated from the standard models to available experimental data. Motivated by the fact that the currently accepted standards for the thermodynamic properties of hydrogen were based on experimental and correlation work completed before the mid-1980s, an assessment of the accuracy of property values for analysis and design of new systems at high and low temperatures and pressures is provided. Property values measured and published after the completion of the current standards for both normal hydrogen and parahydrogen are included in the comparisons. Recommendations for new experimental data needed and for new thermodynamic property formulations for normal hydrogen and parahydrogen are included.

2.1 Methods

In the first experiment on the accurate experimental (p, r, t) data of natural gas mixtures for the assessment of reference equations of state when dealing with hydrogen-enriched natural gas, the volumetric (p, r, T) data were recorded with a single sinker densimeter with magnetic suspension coupling. That method operates on the Archimedes' principle. A magnetic suspension coupling system enables to determine the buoyancy force on a sinker immersed in the medium so that density values over a large range of temperature and pressure can be measured with high accuracy [1]. The design had been adapted and optimized for density measurements of both pure gases and gaseous mixtures. The sinker used here had a cylindrical shape and was made of silicon with a mass of 61.59181 ± 0.00016 g and a corresponding volume of 26.444 ± 0.003 cm3 (k=2), determined at T =293.05 K and p=1.01134 bar. The device operated with a load compensation system that consisted of two calibrated masses made of tantalum and titanium, respectively, that have approximately the same volume (4.9 cm3) but different masses. Mass and volume of these mass pieces underwent a calibration. The weight difference of both masses resembles that of the sinker. The characteristic

load compensation allows for running the measurements near the zero point of the balance where the effect of air buoyancy becomes negligible. Density is calculated using the equation

$$\rho = \frac{\left(m_{so} - m_{sf}\right)}{V_S(T,p)} \qquad (Eq\ 1),$$

where the numerator represents the buoyancy force that is exerted on the sinker. The mass mS0 stands for the weighing result of the sinker in vacuum, mSf for the corresponding result in a pressurized medium. To achieve a higher accuracy, evaluation of data from the single-sinker technique requires a correction for two effects that occur, i.e., the force transmission error (FTE) due to magnetic coupling [2] and absorption of gas molecules on the surface inside the cell and sinker [3]. The FTE is a combination of two effects, namely an apparatus effect and a medium-specific effect. The apparatus effect can be eliminated by simply determining the sinker mass in vacuum mS0 after finishing an isotherm. However, the medium-specific effect results from the magnetic susceptibilities (c) of the mixtures. Literature recommends a consideration only for strongly paramagnetic fluids [2], such as oxygen or oxygen mixtures. The low susceptibility values of the studied gas mixtures in conjunction with the low density of the silicon sinker make a medium-specific correction negligible that was therefore discarded. The influence of sorption effects inside the measuring cell is less defined and thus more difficult to specify due to particular interactions between the medium and the surface. Other researchers working with similar techniques reported errors in density up to 0.1% from such phenomena [3]. The best and approved way to minimize that effect is a procedure of several alternating flushing and evacuating the measuring cell before the actual measurement is started. The residence time inside the cell of the mixture to be investigated did never exceed a period of 40 h. Another viable way to obtain more information on those sorption effects was a specific sorption test for the particular gas mixture in the same way as executed in previous studies [4,5].

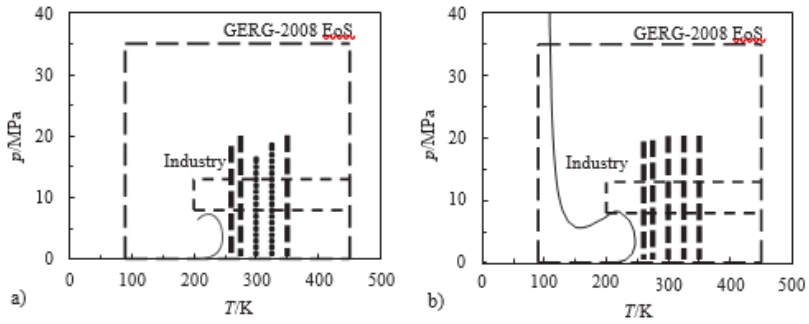

Figure 1 These phase diagram showing the experimental points measured (●) and the calculated saturation curve for the a) 11 M natural gas-like mixture and b) H_2-enriched natural gas mixture. The marked temperature and pressure ranges represent the validity of the GERG-2008 EoS (dashed line) and the area of interest for the transport and compression of gas fuels (thin dashed line).

The volumetric (*p*, r, *T*) data were recorded as isotherms. Both mixtures were investigated at temperatures of 260, 275, 300, 325, and 350 K and up to a maximum pressure of 20 MPa. Fig 1 illustrates the recorded data as coordinates in a *p*, *T*-diagram together with the saturation curve calculated using the GERG- 2008 EoS [6]. The *p*, *T*-range where the GERG-2008 EoS can be applied, and the region of technical relevance are also shown in fig. 1. To ensure an error-free operation of the device, nitrogen as a reference fluid was investigated at selected conditions over the entire operational range [5]. During a measurement, the pressure was reduced in intervals of 1 MPa starting from 20 MPa down to 1 MPa for each isotherm. Here, the established and well regarded GERG-2008 EoS46 was used to predict phase behavior and density of gas mixtures relevant to hydrogen storage, covering the thermodynamic properties of gas phase, liquid phase, and supercritical regions. This equation is valid over a wide range of pressures and temperatures for 21 gas components including 1-methane, 2-nitrogen, 3-carbon dioxide, 4-ethane, 5-propane, 6-n-butane, 7-iso-butane, 8-n-pentane, 9-isopentane, 10-n-hexane, 11-n-heptane, 12-n-octane, 13-hydrogen, 14-oxygen, 15-carbon monoxide, 16-water, 17-helium, 18-argon, 19-n-nonane, 20-n-decane, and 21-hydrogen sulphone.

No.	System: H2 (1st component) + X (2nd Component and beyond)	property type	Pressure Range (Mpa)	Temperature range (K)	X1 range (1st component liquid mole fraction)	Y1 range (1st component gasmole fraction)
1	CH4	VLE/Solubility/Density/Viscosity/Compressibility/Thermal Conductivity	0.22-141.40	66.89-350.00	0.002-0.859	0.034-1.000
2	C2H6	VLE/Compressibility	0.27-562.50	83.00-283.15	0.002-0.800	0.085-1.000
3	C3H8	VLE/Compressibility	0.69-55.16	93.15-366.40	0.001-0.669	0.110-0.999
4	C4H10	VLE/Solubility	2.07-53.43	144.26-394.25	0.008-0.341	0.213-0.999
5	C5H12	VLE/Solubility	0.69-27.59	273.15-463.15	0.004-0.259	0.373-0.997
6	C6H14	VLE/Solubility	1.24-68.95	277.59-506.48	0.011-0.700	0.100-0.998
7	Cyclo-C6H14	VLE/Solubility	0.10-69.04	293.15-523.15	0.000-0.367	0.549-0.997
8	N2	VLE/Solubility/Heat Capacity/Compressibility	0.13-101.33	20.10-122.04	0.012-0.620	0.082-1.00
9	CO2	VLE/Viscosity/Density/Thermal conductivity	0.93-191.80	219.90-298.15	0.001-0.744	0.043-0.934
10	H2S	Solubility	1.01-5.07	243.15-273.15	0.002-0.020	0.322-0.910
11	CO	VLE/Viscosity/Thermal conductivity/Density	0.13-5.07	20.10-122.04	0.012-0.731	0.082-1.00
12	CH4+C2H6	VLE	0.27-562.50	83.00-283.15	0.002-0.800	0.085-1.000
13	C3H8+CO	VLE	0.69-20.68	88.15-348.15	0.005-0.107	0.034-0.847
14	CH4+CO2	VLE	6.90-27.60	227.35-258.15	0.004-0.259	0.373-0.997
15	CH4+CO	VLE	2.90-5.00	120.00-140.00	0.000-0.110	0.000-0.926
16	C5H12+CO2	VLE	6.90-27.60	273.15-323.15	0.004-0.259	0.373-0.997
17	N2+CO	VLE	0.003-22.80	58.15-122.04	0.012-0.930	0.082-1.00
18	CH4+N2	VLE	3.40-10.00	80.00-144.00	0.009-0.720	0.060-1.00

Table 2- gas components

The thermodynamic properties of the fluids, that are predicted here at certain temperatures (T), are based on a multi-fluid approximation using the dimensionless Helmholtz energy obtained from:

$$\alpha(\delta,\tau,\chi) = \alpha^0(\rho,T,\chi) + \alpha^r(\delta,\tau,\chi) \qquad (2)$$

where ρ is the mixture density and χ is the molar composition vector. The term $\tau = \frac{T}{T_r}$ is the inverse reduced temperature, and the term is the reduced density, both of which are composition-dependent i.e. they depend on the molar composition vector. The ideal-gas contribution (α^o) is related to the number of mixture components (N), the mole fraction of each component i (χ_i), and the dimensionless Helmholtz energy of component i in the ideal-gas phase ($\alpha^o{}_{oi}$) by:

$$\alpha^0(\rho,T,\chi) = \sum_{i=1}^{N} x_i\,[\alpha_{oi}^{o}(\rho,T) + \ln x_i] \quad (3)$$

The residual part of the dimensionless Helmholtz energy (α^r) is composed of two different parts; the linear summation of the residual part of the reduced Helmholtz free energy of each component i (α_{oi}^r) and the so-called departure function ($\Delta\alpha^r$) which is also a function of the mixture composition, the inverse reduced mixture temperature, and the reduced mixture density. The residual part of the dimensionless Helmholtz energy is given by:

$$\alpha^r(\delta,\tau,\chi) = \sum_{i=1}^{N} x_i \alpha_{oi}^r\,(\delta,\tau) + \Delta\alpha^r\,(\delta,\tau,\chi) \quad (4)$$

The advantage of using Helmholtz energy in the given form is that all the other thermodynamic properties can be derived analytically from terms α° and α^r and their derivatives. One example is isobaric heat capacity which is given by:

$$c_p(\delta,\tau,\chi) = R[\,-r^2(\alpha_{\tau\tau}^{\circ} + \alpha_{\tau\tau}^{r}) + \frac{(1+\delta\alpha_{\delta}^{r} + \delta\tau\alpha_{\delta\tau}^{r})^2}{1+2\,\delta\alpha_{\delta}^{r} + \delta^2\alpha_{\delta\delta}^{r}}] \quad (5)$$

where R is the gas constant. The subscriptions of α° and α^r denote the order of their derivatives with respect to τ and δ. For example, $\alpha_{\tau\tau}^{\tau}$ denotes the second-order derivatives of αr with respect to τ. Similarly, enthalpy (h), entropy (s), Gibbs free energy (g), pressure (P) can be obtained from:

$$P(\delta,\tau,\chi) = RT_P[1 + \delta\alpha_\delta^r] \quad (6)$$

$$h(\delta,\tau,\chi) = RT[1 + \tau(\alpha_\tau^\circ + \alpha_\tau^r) + \delta\alpha_\delta^r] \quad (7)$$

$$s(\delta,\tau,\chi) = R[\tau(\alpha_\tau^\circ + \alpha_\tau^r) - \alpha^\circ + \alpha^r] \quad (8)$$

$$g(\delta,\tau,\chi) = RT[1 + \alpha_\tau^\circ + \alpha_\tau^r + \delta\alpha_\delta^r] \quad (9)$$

Other thermodynamic properties such as compression factor, internal energy, speed of sound, Joule-Tomson coefficient, etc. can be defined similarly. Kunz. et al. [7] provides comprehensive coverage of these derivatives and thermodynamic properties. In GERG-2008 EoS, terms ρ_r and T_r are calculated using quadratic mixing rules proposed by Klimeck [8]:

$$\frac{1}{p_\tau(x)} = \sum_{i=1}^{N} x_i^2 \frac{1}{p_{c,i}} + \sum_{i=1}^{N-1}\sum_{j=i+1}^{N} \frac{2x_i x_j}{p_{c,ij}} \quad (10)$$

$$T_r(x) = \sum_{i=1}^{N} x_i^2 T_{c,i} + \sum_{i=1}^{N-1}\sum_{j=i+1}^{N} 2x_i x_j T_{c,ij} \quad (11)$$

where $\rho_{c,i}$, is the critical density of component i, is the critical temperature of component i. The parameters for the components studied in this study are provided in figshare entry [9]. $T_{c,ij}$, and $\rho_{c,ij}$are obtained from:

$$\frac{1}{p_{c,ij}} = \beta_{v,ij}\gamma_{v,ij} \frac{x_i + x_j}{\beta_{v,ij}^2 x_i + x_j} * \frac{1}{8}\left(\frac{1}{p_{c,i}^{\frac{1}{3}}} + \frac{1}{p_{c,j}^{\frac{1}{3}}}\right)^3 \quad (12)$$

where $\beta_{v,ij}$, $\gamma_{v,ij}$, $\beta_{T,ij}$,and $\gamma_{T,ij}$ are the four adjustable binary interaction parameters. The binary interaction parameters used for the components in this study are provided in fig share entry [9]. An example of the calculated densities and isobaric heat capacity for H2+CH4 mixtures over a range of pressure and temperature for various H2 mole fractions is provided in Figs. 2 and 3, respectively. Plots of the other derived thermodynamic properties of H2 with CH4 and the thermodynamic properties of H2 with CO2, N2, and the typical natural gas are presented in fig share entry [9].

For calculating viscosity of the system, it was used SuperTRAPP model [10] that is based on the corresponding-states model. SuperTRAPP viscosity model is composed of a dilute-gas and residual

contribution part, where only the latter is treated with corresponding states. The viscosity (μ) is a function of density and pressure and is obtained from:

$$\mu(T,\rho) = \mu^{*}(\mathrm{T}) + \Delta\mu_0(\mathrm{T}_0,\rho_0)\,\mathrm{F}_{\mu}(\mathrm{T},\rho) \qquad (13)$$

where * refers to dilute gas and 0 refers to a reference fluid. The dilute gas viscosity is calculated using Chung et al. [11] theory which is a modification of the original model by Chapman-Enskog [12]. The function F_{μ} can be obtained from:

$$\mathrm{F}_{\mu}(\mathrm{T},\rho) = \sqrt{f}\,h^{-2/3}\sqrt{\frac{m}{m_0}} \qquad (14)$$

To calculate the thermal conductivity of the fluids (γ) they also used SuperTRAPP model [10]. The thermal conductivity is obtained from:

$$\gamma\,(T,p) = \gamma^{int}(T) + \gamma^{*}(T) + \gamma^{r}(T,p) + \gamma^{crit}(T,p) \qquad (15)$$

This method is based on the Ely and Hanley procedure [13] for calculating the thermal conductivity, where the model considers the effect of collisions between molecules (translational energy transfer) (γ^{trans}), and the internal motions of the molecules (γ^{int}, calculated using modified Eucken correlation). The former term can be further divided into three contributions i.e. dilute gas (γ^{*}), residual (γ^{r}) and critical enhancement (γ^{crit}). They refer the reader to the article by Huber ([0] for detailed formulation and parameters of the thermal conductivity. An example of the calculated thermal conductivities for H2+CH4 mixtures over a range of pressures and temperatures for various H2 mole fractions is provided in Fig. 4. The plots of thermal conductivity of H2 with CO2, N2, and the typical natural gas are presented in figshare entry [9].

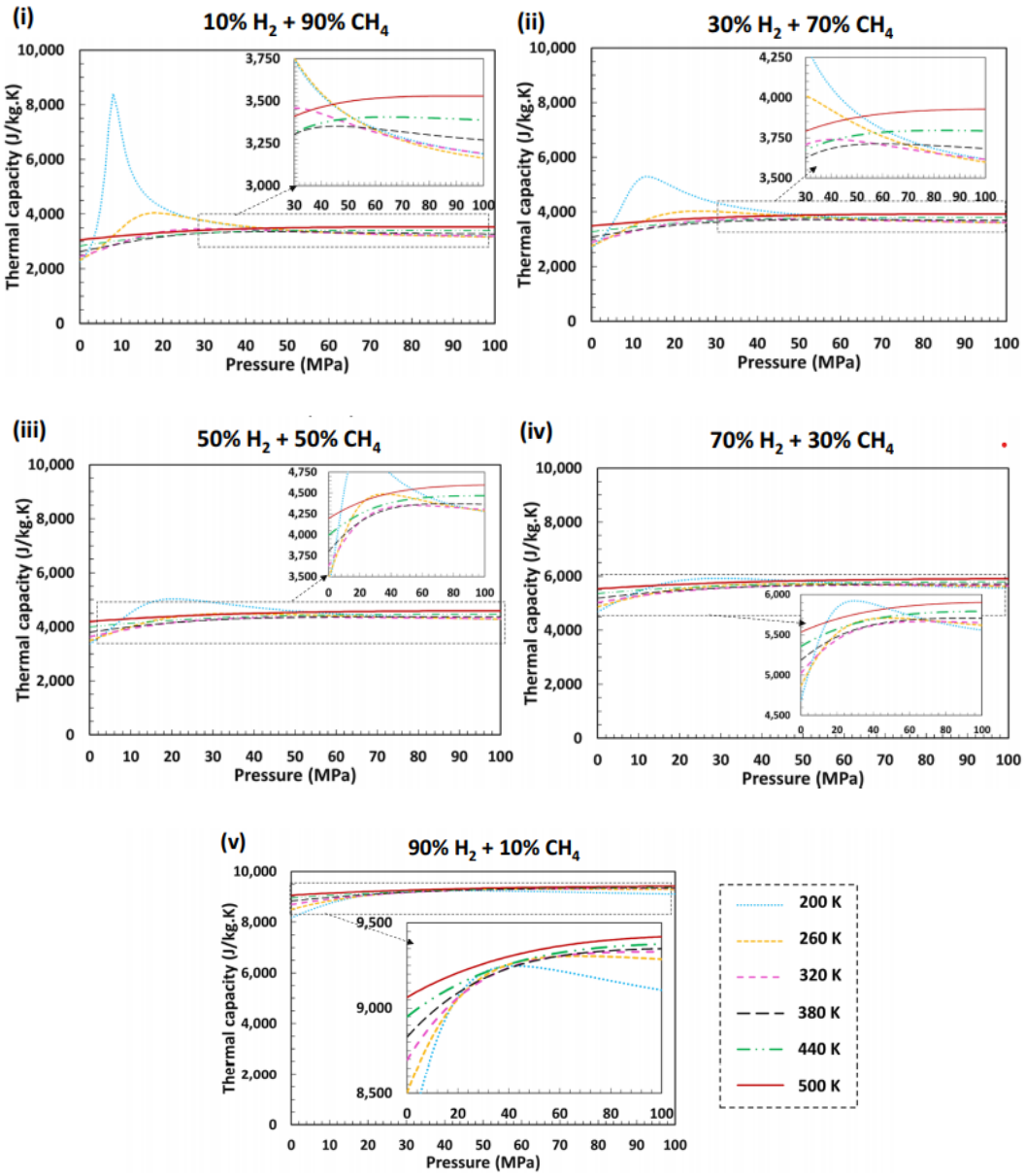

Figure 2-Figure 3-Figure 4-Figure 5-Figure 6

Fig. 5 Predicted isobaric heat capacities for different H2+CH4 mixtures for various H2 mole fractions over a wide range of pressures and temperatures using GERG-2008 EoS. Thermal capacities have higher values for higher H2 mole fractions as the heat capacity of pure H2 is significantly higher than that of pure CH4 at temperatures and pressures above the critical point of CH4. The peaks in the graphs can be attributed to the fact that near the critical points of the components the heat capacities undergo sudden changes because of the changes in their phase. In these examples, as the temperatures and pressures are close to the critical conditions of CH4, peaks have emerged. Reducing the mole fraction of CH4 in the system composition moves the system away from the critical point and as such the peaks reduce or do not appear in the graphs (iv and v). In the third experiment Hydrogen has found applications in fuel cells, food industry, metal production,

pharmaceuticals, aerospace, electronics and power generation. Hydrogen has been produced primarily using steam reforming of natural gases and oil mixtures [14–16]. Recent investigations have been focused on the reforming of ethanol [17] and glycerol [18] as well. Accurate predictions of hydrogen properties are important for product and process design. Equally important are the equations of state (EoSs) that predict the properties of hydrogen and mixtures containing hydrogen. Hydrogen is a low molecular weight substance. At low temperatures and high densities, hydrogen exhibits quantum behavior. It means that in certain applications, e.g. cryogenics, EoSs must appropriately be modified to take into account the impact of the quantum behavior [19]. However, remote from this region, where most applications of hydrogen are carried out, hydrogen shows classical behavior. Hydrogen properties were predicted/correlated using theoretical EoSs [20,21]. Ibrahimoglu et al. [22] analyzed pressure– density and temperature–volume diagrams for hydrogen. Appropriate EoSs for predicting hydrogen properties were also developed, e.g. see Ref. [23]. Moreover, molecular simulation techniques for predicting hydrogen solubility in hydrocarbons, where hydrogen finds applications in hydrogenation coal liquefaction and hydro treatment processes, were performed successfully [24]. Hydrogen solubility in liquid hydrocarbons was also calculated successfully using cubic EoSs [25,26]. In fact, cubic EoSs are conveniently used in engineering applications. Yang [27] used a multi parameter EoS fitted to experimental data in thermodynamic analysis of refueling of a hydrogen tank. Hadj-Kali et al. [28] used the cubic Peng–Robinson (PR) [29] EoS to evaluate the phase equilibria of HIx (H2O–HI–I2) system. The system HIx was also studied by Paricaud et al. [30] using statistical associating fluid theory with variable range (SAFT-VR) [31]. Mohamed and Paraschivoiu [32] used the Beattie–Bridgeman EoS [33] to assess the high-pressure behavior of hydrogen when released from a chamber. Schouten et al. [34] used the PR EoS to amount the condensation of a natural gas in transmission pipelines. The non-isothermal behavior of compressible natural gases mixed with hydrogen in pipelines was analyzed by Uilhoorn [35] using the Predictive Soave–Redlich–Kwong (PSRK) EoS [36]. Absorption properties of hydrogen including fugacity and compressibility factor of hydrogen were evaluated by Zhou and Zhou [37] using the Redlich–Kwong–Soave (RKS) [38] and Benedict–Web–Rubin (BWR) EoSs [39]. The RKS EoS was used at 30 bar and high temperatures by Aktasx et al. [40] in thermodynamic analysis of steam assisted conversion of bio-oil components to synthesis gases. Zheng et al. [41] and Yang and Huber [42] used NIST data base equation [43] for analyzing processes containing hydrogen. Cubic EoSs are simple, robust and predictive to a certain extent [44,45]. Consequently, cubic EoSs are very popular. However, there are plenty of cubic EoSs in the literature. Excellent reviews of cubic EoSs can be found elsewhere [46–49]. Newly developed EoSs are also emerging. Thus, the accuracy of an EoS

must be tested appropriately before using it in a specific application. Cubic EoSs are generally used to correlate the vapor pressures (and sometimes the liquid densities) of pure substances and predict other properties along the vapor–liquid coexistence curve. Far from the critical point, the accuracies of cubic EoSs in predicting the supercritical properties are not clear; however. In this work they evaluate the accuracies of eleven cubic EoSs in predicting the saturated and supercritical properties of hydrogen for wide ranges of temperature and pressure. For accurate prediction of hydrogen properties, the alpha functions and PVT relationships of EoSs are equally important. Therefore, in addition to the widely used RKS EoS [38], PR EoS [29] and Patel–Teja (PT) EoS [50], some of the most successful variants of these EoSs are used. Are introduced developments of Eos [51]. However, they do not use theoretical EoS in our evaluations as these EoSs are often used for chain, associating molecules and electrolytes. Then, they attempt to predict the saturated properties of hydrogen (vapor pressure, saturated liquid and vapor densities, enthalpies and entropies of vaporization, and saturated liquid and vapor heat capacities at constant pressure) using the eleven EoSs. Afterwards, the second virial coefficients, compressibility factors, enthalpies, entropies, constant pressure heat capacities, speeds of sound, Joule–Thomson coefficients and inversion curves of hydrogen are predicted for wide ranges of temperature and pressure. The accuracies of the EoSs in predicting the properties of hydrogen are compared with experimental data, recommended values of thermodynamic tables and also with each other. The best EoSs among the others for predicting hydrogen properties are introduced, and their accuracies are reported. The fourth experiment tells us that the process gas of ethylene plants and methyl tertiary butyl ether plants is normally a hydrogen/methane mixture. The molecular weight of the gas in such processes ranges from 3.5 to 14. Thermodynamic behavior of hydrogen/methane mixture has been and is being researched extensively. The gas dynamic design of turboexpanders which are extensively utilized in such plants depends on the equations of state of the process gas. Optimum performance of the turboexpander and associated equipment demands accurate thermodynamic properties for a wide range of process gas conditions. The existing equations of state, i.e. Benedict-WebbRubin (BW R), Soave-Redlich-Kwang and PengRobinson have some practical limitations. The field data collected for hydrogen/methane mixtures are in the range of 100°F to -200°F containing some polar components i.e. H2S and CO2. In the fifth experiment the data for the thermodynamic properties of normal hydrogen and parahydrogen are listed in Tables 3 and 4. P-ρ-T and speed-of-sound data for normal hydrogen are illustrated in Figs. 2 and 3, and those for parahydrogen are illustrated in Figs. 4 and 5. Included are comparisons to data above 400 K (even though the range of applicability of the formulations is exceeded) to illustrate the extrapolation behaviour of the formulations. Data at

temperatures below 240 K require a specification of the orthohydrogen–parahydrogen concentration to characterize the sample because the equilibrium concentration differs from the “normal” 75–25 ratio, so that a sample in equilibrium at room temperature would change composition over time. Data published before 1933 were measured before the existence of orthohydrogen and parahydrogen had been established and are compared here to the normal hydrogen equation of state even though the true concentration of the measured samples is uncertain. While most data sets after 1933 estimate a sample concentration prior to taking data, the concentration of each data point for hydrogen that is not at equilibrium is generally not given and can vary throughout the measurements.

Author	Year	Number of points	Temperature range (K)	Pressure range (MPa)	Absolute average deviation (%)
P-ρ-T					
Bartlett	1927	8	273.2	5.1–101.3	0.37
Bartlett et al.	1928	43	273.2–673.0	5.1–101.3	0.29
Bartlett et al.	1930	54	203–293	2.6–102.7	0.38
David and Hamann	1953	12	65–79	30.4–126.7	0.53
Golubev and Dobrovolskii	1964	31	33.2–77.4	4.8–47.6	1.03
Holborn and Otto	1925	30	65.25–223.1	2.0–10.0	0.17
Jaeschke and Humphreys					
Gasunie	1990	68	273.2–353	0.2–26.3	0.04
Ruhrgas	1990	221	273.2–353	0.5–28.1	0.04
Johnston et al.	1954	62	20.3–32.6	0.9–11.9	0.68
Johnston et al.	1953	227	33–300	0.5–20.6	0.69
Liebenberg etal.	1978	19	75.0–163.9	473.3–1871	–
Liebenberg etal.	1977	1953	75–307	200–2,000	4.78
Machado etal.	1988	60	130–159	1.2–105.5	5.16
Michels and Goudeket	1941	283	273–423	0.9–300.9	0.13
Michels et al.	1959	482	98.2–423.2	0.7–299.2	0.11
Scott	1929	18	298	0.10–17.2	0.15
Townend and Bhatt	1931	40	273–298	0.1–60.8	0.11
Tsiklis etal.	1975	45	298.1–423.1	50–650	0.52
Verschoyle	1926	25	273–293	5.0–21.0	0.15
Wiebe and Gaddy	1938	47	273–573	2.5–101.3	0.08
Isobaric heat capacity					
Gutsche	1939	73	16.5–37.5	1.0–9.7	7.95
Speed of sound					
Guesewell etal.	1970	7	25–31	0.1	6.37
Liebenberg etal.	1978	19	75.0–163.9	473.3–1871	–
Liebenberg etal.	1977	1953	75–307	200–2,000	9.30

Matsuishi et al.	2003	42	293–526	1,190–10,840	–
van Dael et al.	1965	175	22.2–33	0.2–24.8	1.82
van Itterbeek etal.	1961	42	14.1–20.4	0.009–0.1	1.69
van Itterbeek etal.	1963	110	15.1–20.5	0.02–23.5	6.37
Vapor pressure					
Aston et al.	1935	4	18.0–20.7	Sat	4.65
Barber	1964	1	13.816	Sat	3.02
Grilly	1951	8	19.3–24.5	Sat	3.53
Henning	1926	25	14.0–20.5	Sat	6.78
Henning and Otto	1936	19	13.93–20.38	Sat	13.11
Hiza	1981	12	20.0–30.0	Sat	2.40
Keesom et al.	1931	31	17.2–20.5	Sat	4.25
Traver and Jaquerod	1902	9	14.9–20.4	Sat	3.53
van Itterbeek etal.	1964	42	20.6–32.3	Sat	3.54
White et al.	1950	17	20.9–33.1	Sat	3.79
White et al.	1950	6	33.08–33.25	Sat	3.33
Author	**Year**	**Number of points**	**Temperature range (K)**	**Pressure range (MPa)**	**Absolute average difference ($cm^3 \cdot mol^{-1}$)**
Second virial coefficient					
Bartlett et al.	1928	5	273.2–572.3		0.52
Beenakker et al.	1959	1	20.4		10.02
Cottrell et al.	1956	1	303.2		1.04
Dehaas	1912	3	289.1–293.7		15.99
El Hadi etal.	1969	7	19.3–26.3		1.48
Gibby et al.	1929	7	298.2–448.2		0.48
Holborn and Otto	1925	8	90.2–473.2		3.05
Holborn and Otto	1926	9	65.3–473.2		11.12
Johnston et al.	1953	18	35.1–300		0.20
Kerl	1982	1	293.1		–

Author	Year	Number of points	Temperature range (K)	Pressure range (MPa)	Absolute average deviation (%)
Knaap et al.	1962	23	20.5–65.0		5.69
Long and Brown	1937	7	20.9–46.5		1.83
Lopatinskii et al.	1991	2	293.2		0.43
Michels and Goudeket	1941	20	273.2–423.2		1.14
Michels et al.	1959	17	98.2–423.2		0.77
Mihara et al.	1977	3	298.2–348.2		0.57
Mueller et al.	1961	6	73.2–323.2		8.85
Nijhoff and Keesom	1927	8	24.84–373.15		1.54
Perez et al.	1980	5	300–500		0.75
Schramm et al.	1991	1	296.2		0.92
Scott	1929	1	298.2		0.45
Townend and Bhatt	1931	2	273.2–298.2		0.60
van Agt and Kamerlingh Onnes	1925	9	14.6–90.3		3.90
Varekamp and Beenakker	1959	8	14.0–21.0		8.87
Verschoyle	1926	2	273.2–293.2		0.44
Wiebe and Gaddy	1938	6	273.2–573.2		0.39
Author	**Year**	**Number of points**	**Temperature range (K)**	**Pressure range (MPa)**	**Absolute average difference ($cm^6 \cdot mol^{-2}$)**
Third virial coefficient					
Holborn and Otto [15]	1925	5	90.2–273.2		0.99
Johnston et al. [18]	1953	18	35.1–300.0		0.11
Michels and Goudeket [22]	1941	20	273.2–423.2		0.53
Michels et al. [23]	1959	17	98.2–423.2		0.14
Mihara et al. [56]	1977	3	298.2–348.2		0.12
Scott [24]	1929	1	298.2		0.20

Townend and Bhatt [25]	1931	2	273.2–298.2		0.12
Verschoyle [27]	1926	2	273.2–293.2		0.03

Table 3

Author	Year	Number of points	Temperature range (K)	Pressure range (MPa)	Absolute average deviation (%)
P-ρ-T					
Goodwin et al.	1963	1,234	15–100	1.5–35.5	0.87
Goodwin et al.	1961	17	17.0–33.0	Sat	0.02
Hoge and Lassiter	1951	46	32.9–33.3	1.3–1.4	4.41
Roder et al.	1963	46	33.0–40.0	1.3–2.8	2.33
Isochoric heat capacity					
Younglove and Diller	1962	162	19.9–90.4	1.1–63.3	1.24
Isobaric heat capacity					
Medvedev et al.	1971	319	20.9–50.3	0.2–3.0	4.56
Speed of sound					
Younglove	1965	251	14.5–100.0	Sat-32.0	1.58
van Itterbeek etal.	1961	48	14.1–20.4	Sat	2.88
van Itterbeek etal.	1963	116	15.1–20.5	Sat-23.5	1.52
van Dael et al.	1965	23	20.3–32.0	Sat	4.25
Vapor pressure					
Barber and Horsford	1963	10	13.8–20.3	0.007–1.2	0.20
Hoge and Arnold	1951	45	15.8–32.9	0.02–1.2	0.16
Keesom et al.	1931	31	17.2–20.5	0.1	1.12
van Itterbeek etal.	1964	42	20.6-32.3	0.1–1.2	0.86
Weber etal.	1962	32	20.3–32.7	0.1–1.2	0.32
Saturation heat capacity					
Brouwer et al.	1970	12	24.5–30.0	Sat	0.73
Smith et al.	1954	8	18.3–31.5	Sat	1.04
Johnston et al.	1950	16	12.7–19.0	Sat	2.45
Younglove and Diller	1962	32	14.8–31.5	Sat	2.73
Author	**Year**	**Number of points**	**Temperature range (K)**	**Pressure range (MPa)**	**Absolute average difference ($cm^3 \cdot mol^{-1}$)**

Second virial coefficient					
Goodwin et al. [77]	1964	58	15.0–423.2		0.78
Author	**Year**	**Number of points**	**Temperature range (K)**	**Pressure range (MPa)**	**Absolute average difference ($cm^6 \cdot mol^{-2}$)**
Third virial coefficient					
Goodwin et al.	1964	52	20.0–423.2		0.29

Table 4

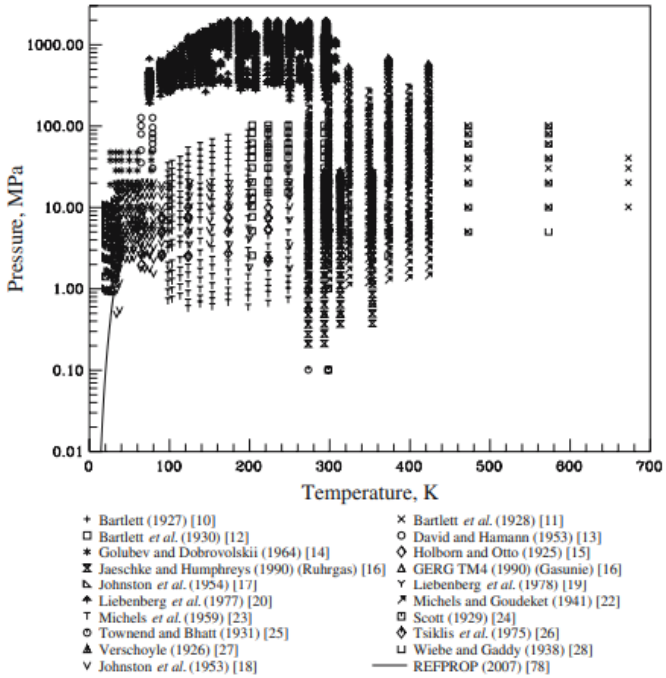

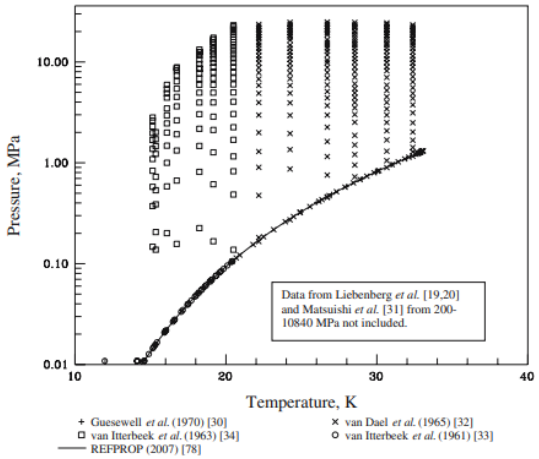

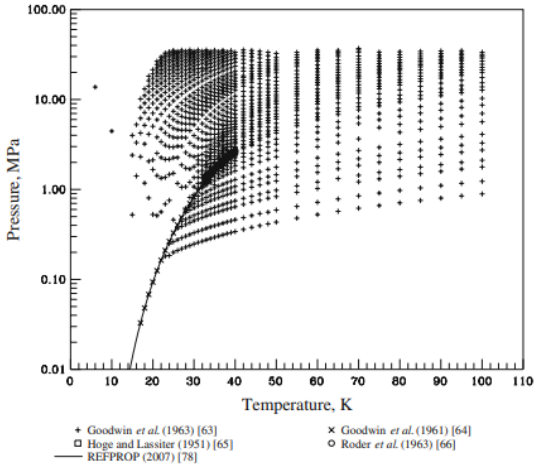

Figure 7-Figure 8-Figure 9

2.2 Details

In the first experiment the uncertainties of the various measurements were analyzed from Roberto Hernandez-Gomez, Dirk Tuma, Daniel Lozano-Martın, Cesar R. Chamorro. The uncertainty in temperature amounted to less than 4 mK, the uncertainty in pressure depended on the range covered by the individual transducer. Eq. (16) gives the uncertainty relation for the high-pressure (3-20 MPa) transducer, and Eq. (17) for the low-pressure transducer (0-3 MPa), respectively. The uncertainty in pressure in both mixtures remained below 0.005 MPa.

$$U(\mathrm{p})/\mathrm{MPa} = 75\cdot10^{-6}\cdot p\,/\,\mathrm{MPa} + 3.5\cdot10^{-3} \quad (16)$$

$$U(\mathrm{p})/\mathrm{MPa} = 60\cdot10^{-6}\cdot p\,/\,\mathrm{MPa} + 1.7\cdot10^{-3} \quad (17)$$

The uncertainty of the density value was calculated by executing the uncertainty propagation law on Eq. (16) according to the procedures given in the Guide to the Expression of Uncertainty in Measurement (GUM) [52]. From Eq. (16), the true sinker mass mS0, the apparent sinker mass in the medium mSf, and the sinker volume VS (T, p) contribute to the uncertainty. Additionally, the uncertainty of the apparent sinker mass mSf includes the entry from calibration, resolution, repeatability, and balance drift. Since the sinker volume VS is affected by temperature and pressure, Eq. (18) describes the effect of thermal expansion and pressure distortion as a function of density.

$U(p) / kg \cdot m^{-3} = 1.1 \cdot 10^{-4} \cdot p/kg \cdot m^{-3} + 2.3 \cdot 10$ (18)

The overall expanded uncertainty in density UT (p) includes the uncertainties of density, temperature, pressure, and ultimately the composition of the gas mixture, see Eq. (19).

$$U_T(\rho) = 2 * [u(p^2) + \left(\left(\frac{\partial \rho}{\partial p}\right)_{T,x} * u(p)\right)^2 + \left(\left(\frac{\partial \rho}{\partial T}\right)_{p,x} * u(T)\right)^2 + \sum_i \left(\left(\frac{\partial \rho}{\partial x_i}\right)_{T,p,x_j \neq x_i} * u(x_i)\right)^2]^{0.5} \quad (19)$$

In Eq. (19), apart from temperature T and pressure p, xi is the amount-of-substance (mole) fraction of each individual mixture component. Partial derivatives of Eq. (19) may be calculated from GERG-2008 EoSe via REFPROP [53].

T/K	p/Mpa	ρ_{exp}/kg·m^{-3}	U (ρ_{exp})/kg·m^{-3} (k=2)	10^2 U (ρ_{exp})/ρ_{exp}	10^2 (ρ_{exp}-ρ_{GERG})/ρ_{GERG}	10^2 (ρ_{exp}-ρ_{AGA})/ρ_{AGA}
259.989	17.977	225.658	0.049	0.022	—0.065	—0.127
259.992	17.023	216.671	0.048	0.022	—0.074	—0.119
259.994	16.014	206.202	0.047	0.023	—0.084	—0.109
259.992	15.025	194.876	0.045	0.023	—0.092	—0.100
259.994	14.012	182.092	0.044	0.024	—0.095	—0.093
259.995	13.021	168.450	0.042	0.025	—0.090	—0.093
259.994	12.009	153.491	0.041	0.027	—0.075	—0.099
259.994	11.014	138.040	0.039	0.028	—0.047	—0.098
259.996	10.013	122.146	0.037	0.030	—0.025	—0.099

259.990	9.008	106.300	0.035	0.033	—0.007	—0.096
259.993	7.988	90.764	0.034	0.037	0.010	-
259.991	7.000	76.503	0.032	0.042	0.020	—0.077
259.992	5.999	62.980	0.030	0.048	0.019	—0.075
259.992	4.998	50.417	0.029	0.057	0.015	—0.072
259.993	4.002	38.839	0.028	0.071	0.008	—0.068
259.994	2.997	28.021	0.026	0.094	0.005	—0.059
259.992	1.992	17.972	0.025	0.140	—0.001	—0.048
259.991	0.998	8.701	0.024	0.278	—0.013	—0.041
274.977	19.622	213.256	0.048	0.022	—0.057	—0.117
274.977	19.015	208.165	0.047	0.023	—0.061	—0.114
274.975	17.999	199.103	0.046	0.023	—0.067	—0.108
274.976	17.010	189.597	0.045	0.024	—0.071	—0.102
274.976	16.002	179.179	0.044	0.024	—0.072	—0.099
274.973	14.994	168.038	0.042	0.025	—0.071	—0.099
274.971	14.005	156.441	0.041	0.026	—0.065	—0.100
274.972	13.007	144.175	0.040	0.027	—0.056	—0.102
274.972	12.009	131.463	0.038	0.029	—0.044	—0.100
274.971	11.007	118.489	0.037	0.031	—0.027	—0.092
274.972	10.004	105.462	0.035	0.033	—0.018	—0.090
274.971	9.001	92.621	0.034	0.036	—0.010	—0.087
274.971	8.000	80.158	0.032	0.040	—0.005	—0.085
274.971	7.001	68.196	0.031	0.045	0.001	—0.079
274.972	5.998	56.751	0.030	0.052	0.003	—0.075
274.972	4.997	45.910	0.028	0.062	0.002	—0.070
274.972	4.001	35.703	0.027	0.076	—0.001	—0.064
274.971	3.000	26.006	0.026	0.101	—0.003	—0.054
274.968	2.000	16.860	0.025	0.149	<0.001	—0.038
274.969	0.998	8.183	0.024	0.295	0.001	—0.021
299.934	16.303	150.195	0.040	0.027	—0.027	—0.072
299.934	16.008	147.459	0.040	0.027	—0.026	—0.072
299.933	15.003	137.934	0.039	0.028	—0.022	—0.073

299.932	13.999	128.156	0.038	0.030	—0.017	—0.073
299.933	13.000	118.212	0.037	0.031	—0.012	—0.072
299.934	12.000	108.142	0.036	0.033	—0.008	—0.072
299.932	11.001	98.044	0.034	0.035	0.001	—0.065
299.931	10.001	87.967	0.033	0.038	0.002	—0.066
299.930	9.001	78.002	0.032	0.041	0.003	—0.065
299.931	7.999	68.196	0.031	0.045	0.004	—0.064
299.930	6.998	58.628	0.030	0.051	0.004	—0.060
299.926	5.996	49.322	0.029	0.058	0.004	—0.056
299.927	4.998	40.335	0.028	0.069	0.004	—0.049
299.926	3.998	31.645	0.027	0.085	0.001	—0.044
299.928	2.997	23.266	0.026	0.111	0.003	—0.033
299.926	1.997	15.204	0.025	0.164	0.002	—0.025
299.923	0.997	7.446	0.024	0.323	—0.005	—0.021
324.932	18.569	146.171	0.040	0.027	—0.047	—0.099
324.934	18.000	141.876	0.039	0.028	—0.046	—0.100
324.936	16.998	134.140	0.038	0.029	—0.044	—0.102
324.936	15.997	126.218	0.038	0.030	—0.042	—0.104
324.936	14.997	118.150	0.037	0.031	—0.038	—0.103
324.937	13.998	109.947	0.036	0.033	—0.036	—0.102
324.937	12.999	101.654	0.035	0.034	—0.034	—0.101
324.937	11.998	93.287	0.034	0.036	—0.031	—0.099
324.936	10.997	84.908	0.033	0.039	—0.024	—0.090
324.936	10.001	76.578	0.032	0.042	—0.027	—0.091
324.935	8.998	68.248	0.031	0.045	—0.025	—0.087
324.933	7.997	60.023	0.030	0.050	—0.023	—0.082
324.933	6.997	51.928	0.029	0.056	—0.021	—0.075
324.934	5.997	43.970	0.028	0.064	—0.022	—0.070
324.934	4.997	36.174	0.027	0.076	—0.023	—0.065
324.934	3.997	28.555	0.026	0.093	—0.022	—0.057
324.934	2.997	21.122	0.026	0.121	—0.023	—0.051
324.930	1.990	13.831	0.025	0.179	—0.023	—0.044

324.929	0.998	6.837	0.024	0.351	—0.032	—0.044
349.919	19.701	136.343	0.039	0.028	—0.031	—0.095
349.918	18.999	131.749	0.038	0.029	—0.030	—0.096
349.918	17.997	125.065	0.037	0.030	—0.029	—0.098
349.919	16.995	118.246	0.037	0.031	—0.027	—0.098
349.919	15.997	111.336	0.036	0.032	—0.026	—0.098
349.921	14.996	104.305	0.035	0.034	—0.024	—0.096
349.920	13.996	97.202	0.034	0.035	—0.023	—0.094
349.919	12.995	90.022	0.033	0.037	—0.022	—0.092
349.919	11.997	82.823	0.033	0.039	—0.021	—0.089
349.918	10.999	75.612	0.032	0.042	—0.018	—0.082
349.919	9.997	68.368	0.031	0.045	—0.019	—0.079
349.919	8.996	61.155	0.030	0.049	—0.020	—0.076
349.919	7.996	53.989	0.029	0.054	—0.021	—0.072
349.918	6.997	46.892	0.029	0.061	—0.019	—0.065
349.918	5.996	39.864	0.028	0.070	—0.021	—0.061
349.918	4.997	32.935	0.027	0.082	—0.022	—0.057
349.918	3.996	26.095	0.026	0.100	—0.025	—0.055
349.918	2.998	19.395	0.025	0.131	—0.026	—0.050
349.917	1.997	12.791	0.025	0.193	—0.020	—0.037
349.917	0.997	6.323	0.024	0.378	—0.031	—0.042

Table 5- Experimental (p,ρ, T) measurements for the 11 M (BAM-G 420) natural gas, relative and absolute expanded uncertainty in density (k=2) U (ρ_{exp}), and relative deviations from the GERG-2008 and AGA8-DC92 EoS; where T is the temperature (ITS-90), p the pressure, ρ_{exp} the experimental density, and ρ_{GERG} and ρ_{AGA} the densities calculated from the GERG-2008 and the AGA8-DC92 EoS.

The experimental volumetric (p, r, T) data measured for the two natural gas mixtures during this work are given in Table 5 for the 11 M (BAM-G 420) mixture and Table 6 for the H2- enriched mixture together with the corresponding expanded uncertainty in density from Eq. (18) and expressed both in density units (kg m^-3 , i.e., absolute value) and as percentage of the measured density (i.e., relative value). The experimental data were compared to the corresponding density data calculated

from the GERG-2008 and AGA8-DC92 EoS. Two columns in the Tables 5 and 6 represent the relative deviations between experimental and calculated data.

T/K	p/Mpa	ρ_{exp}/kg·m^{-3}	U (ρ_{exp})/kg·m^{-3} (k=2)	10^2 U (ρ_{exp})/ρ_{exp}	10^2 (ρ_{exp}-ρ_{GERG})/ρ_{GERG}	10^2 (ρ_{exp}-ρ_{AGA})/ρ_{AGA}
260.041	19.843	224.730	0.049	0.022	—0.254	—0.193
260.038	19.011	217.428	0.048	0.022	—0.268	—0.178
260.040	18.010	208.053	0.047	0.023	—0.280	—0.156
260.041	17.008	197.993	0.046	0.023	—0.288	—0.133
260.040	16.010	187.277	0.045	0.024	—0.291	—0.114
260.040	15.012	175.878	0.043	0.025	—0.285	—0.097
260.040	14.011	163.801	0.042	0.026	—0.269	—0.083
260.039	13.012	151.191	0.040	0.027	—0.245	—0.071
260.038	12.011	138.130	0.039	0.028	—0.214	—0.063
260.039	11.009	124.803	0.037	0.030	—0.171	—0.051
260.041	10.008	111.413	0.036	0.032	—0.135	—0.050
260.040	9.005	98.132	0.034	0.035	—0.104	-
260.041	8.010	85.247	0.033	0.039	—0.075	—0.059
260.040	7.007	72.690	0.031	0.043	—0.050	—0.060
260.040	6.001	60.600	0.030	0.050	—0.035	—0.064
260.038	4.999	49.124	0.029	0.059	—0.025	—0.064
260.039	4.001	38.246	0.028	0.072	—0.018	—0.060
260.040	2993	27.840	0.026	0.095	<0.001	—0.039
260.041	1.998	18.098	0.025	0.140	—0.013	—0.045
260.041	0.999	8.815	0.024	0.275	0.001	—0.019
275.020	19.234	196.179	0.046	0.023	—0.225	—0.126
275.019	18.008	185.120	0.044	0.024	—0.228	—0.111
275.018	17.013	175.624	0.043	0.025	—0.226	—0.101
275.018	16.006	165.559	0.042	0.025	—0.220	—0.092
275.016	15.004	155.107	0.041	0.026	—0.209	—0.084

275.017	14.008	144.361	0.040	0.027	—0.193	—0.076
275.016	13.007	133.256	0.038	0.029	—0.174	—0.070
275.015	12.006	121.941	0.037	0.030	—0.155	—0.067
275.015	11.004	110.531	0.036	0.032	—0.128	—0.060
275.013	10.006	99.141	0.035	0.035	—0.111	—0.063
275.014	9.003	87.821	0.033	0.038	—0.092	—0.065
275.013	8.002	76.705	0.032	0.042	—0.076	—0.069
275.013	7.001	65.854	0.031	0.047	—0.060	—0.068
275.013	6.000	55.328	0.030	0.053	—0.049	—0.067
275.013	5.003	45.205	0.028	0.063	—0.038	—0.062
275.012	4.006	35.445	0.027	0.077	—0.027	—0.054
275.011	3.001	26.000	0.026	0.101	—0.012	—0.037
275.011	2.000	16.957	0.025	0.148	—0.003	—0.025
275.011	0.999	8.296	0.024	0.291	0.009	—0.005
299.961	19.851	171.675	0.043	0.025	—0.162	—0.089
299.961	19.009	165.029	0.042	0.025	—0.161	—0.086
299.960	18.003	156.843	0.041	0.026	—0.157	—0.084
299.960	17.002	148.434	0.040	0.027	—0.152	—0.081
299.960	16.003	139.800	0.039	0.028	—0.145	—0.078
299.960	15.002	130.945	0.038	0.029	—0.137	—0.075
299.960	14.002	121.924	0.037	0.030	—0.127	—0.072
299.960	13.003	112.776	0.036	0.032	—0.116	—0.069
299.958	12.003	103.536	0.035	0.034	—0.108	—0.069
299.958	11.000	94.230	0.034	0.036	—0.091	—0.061
299.958	10.002	84.966	0.033	0.039	—0.082	—0.062
299.958	9.001	75.735	0.032	0.042	—0.071	—0.059
299.957	8.000	66.591	0.031	0.046	—0.061	—0.057
299.956	7.002	57.603	0.030	0.052	—0.049	—0.052
299.956	5.999	48.731	0.029	0.059	—0.042	—0.049
299.957	4.999	40.073	0.028	0.069	—0.031	—0.042
299.959	3.998	31.613	0.027	0.085	—0.021	—0.033
299.958	2.991	23.309	0.026	0.111	—0.008	—0.020

299.957	1.999	15.356	0.025	0.162	—0.004	—0.016
299.958	0.999	7.557	0.024	0.318	0.001	—0.007
324.963	19.928	150.681	0.040	0.027	—0.107	—0.064
324.962	19.001	144.143	0.040	0.027	—0.105	—0.065
324.963	17.999	136.914	0.039	0.028	—0.102	—0.064
324.963	17.000	129.541	0.038	0.029	—0.098	—0.063
324.964	16.000	122.027	0.037	0.030	—0.094	—0.061
324.963	14.998	114.372	0.036	0.032	—0.088	—0.059
324.963	14.001	106.647	0.035	0.033	—0.082	—0.056
324.963	13.002	98.826	0.034	0.035	—0.076	—0.054
324.962	12.001	90.934	0.034	0.037	—0.069	—0.051
324.963	11.000	83.015	0.033	0.039	—0.057	—0.042
324.963	9.999	75.089	0.032	0.042	—0.053	—0.042
324.962	8.999	67.186	0.031	0.046	—0.043	—0.036
324.962	7.999	59.321	0.030	0.051	—0.037	—0.033
324.962	6.999	51.523	0.029	0.056	—0.028	—0.027
324.962	5.998	43.796	0.028	0.064	—0.023	—0.025
324.961	4.999	36.180	0.027	0.076	—0.018	—0.022
324.962	3.998	28.673	0.026	0.092	—0.012	—0.018
324.961	2.985	21.199	0.026	0.121	—0.002	—0.009
324.961	1.999	14.050	0.025	0.177	—0.001	—0.008
324.962	0.998	6.945	0.024	0.345	0.005	—0.001
349.946	19.941	134.571	0.039	0.029	—0.110	—0.091
349.946	19.000	128.613	0.038	0.029	—0.108	—0.090
349.945	17.997	122.149	0.037	0.030	—0.106	—0.089
349.946	16.995	115.580	0.036	0.031	—0.102	—0.087
349.944	15.998	108.944	0.036	0.033	—0.099	—0.085
349.946	14.996	102.190	0.035	0.034	—0.094	—0.081
349.946	13.998	95.389	0.034	0.036	—0.089	—0.077
349.945	12.998	88.509	0.033	0.038	—0.085	—0.074
349.944	11.991	81.546	0.032	0.040	—0.073	—0.063
349.945	10.996	74.624	0.032	0.042	—0.064	—0.056

349.945	9.997	67.658	0.031	0.046	—0.062	—0.055
349.946	8.998	60.691	0.030	0.050	—0.057	—0.052
349.947	7.998	53.731	0.029	0.055	—0.052	—0.049
349.947	6.997	46.792	0.029	0.061	—0.045	—0.044
349.947	5.998	39.899	0.028	0.070	—0.041	—0.042
349946	4998	33064	0.027	0.082	—0.037	—0.040
349946	3998	26284	0.026	0.100	—0.032	—0.037
349946	2985	19492	0.025	0.130	—0.026	—0.031
349946	1999	12964	0.025	0.190	—0.025	—0.031
349946	0.999	6431	0.024	0.372	—0.007	—0.012

Table 6-Experimental (p, r, T) measurements for the H_2-enriched natural gas mixture, relative and absolute expanded uncertainty in density (k=2) U (ρ_{exp}), and relative deviations from the GERG-2008 and AGA8-DC92 EoS; where T is the temperature (ITS-90), p the pressure, ρ_{exp} the experimental density, and ρGERG and ρAGA the densities calculated from the GERG-2008 and the AGA8-DC92 EoS.

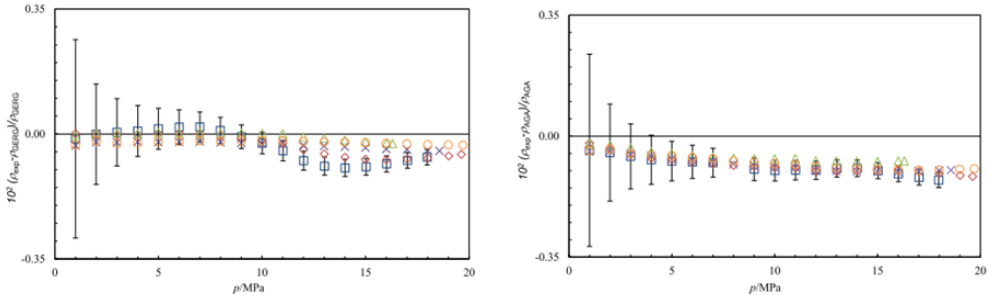

Figure 10 - Figure 11 show the relative deviations of experimental density data from density data calculated by the GERG-2008 (pGERG) and AGA8-DC92 (pAGA) EoS versus pressure p at a constant temperature T for the 11 M natural gas mixture.

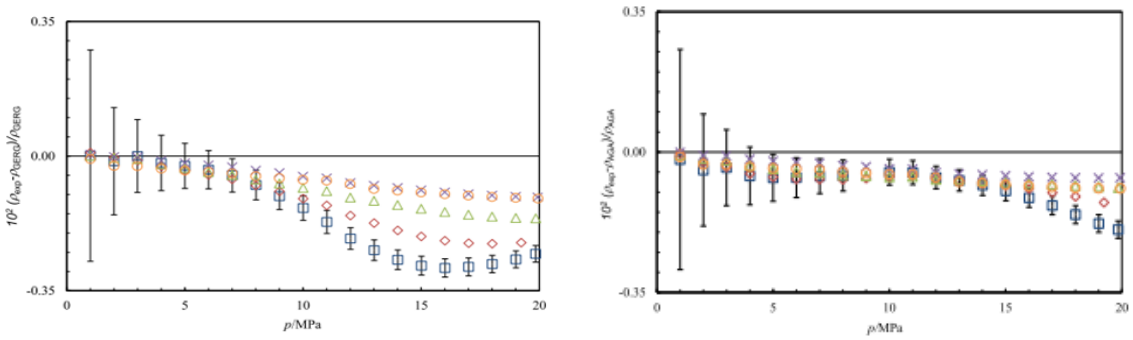

Figure 12-Figure 13 represent the equivalent for the H2-enriched natural gas mixture. The intrinsic uncertainty of the GERG-2008 EoS in the gas phase region over the temperature range from 250 to 450 K and at pressures up to 35 MPa amounts to 0.1% in density

A look at the Figs. 10-13 shows that a negative deviation of the calculated density compared to the experimental density dominates for both gas mixtures and both equation-of-state models. For the 11 M mixture processed by the GERG-2008 EoS shown in Fig. 10, the data follow a relatively flat sinusoid curve, but all data remain within the 0.1-% margin, with the largest deviation for the lowest temperature T=260 K. The deviations are all negative and the deviation increases slowly but monotonously towards increasing pressure. A comparison of the performance of both equation-of-state models shows that GERG-2008 performs better on 11 M than AGA8-DC92, but the gain diminishes when going towards lower temperatures. The results for the H2- enriched gas mixtures are apparently different. The GERG-2008 EoS shown in Fig. 12 resulted in a quite similar pattern as for the 11 M mixture, but more strongly pronounced. The deviation becomes steeper at about 5 MPa and goes through a maximum of about 0.30% at around 16 MPa. There is a visible temperature dependence. In contrast, the AGA8-DC92, shown in Fig. 13, shows a smaller deviation and a less pronounced temperature dependence until a pressure of 15 MPa where a steeper deviation begins. As expected, the performance on the H2-enriched mixture is generally poorer and, surprisingly, the AGA8-DC92 gives better results. The findings illustrated in Figs. 10and13 were further evaluated by statistical parameters that were already applied in previous studies and are given in Table 7. Eq. (20) defines the average absolute deviation AAD, Eq. (21) the so-called Bias that quantifies the average deviation of the data set, and Eq. (22) represents the root mean square RMS. The subscript “EoS” is replaced by “GERG” or “AGA” to denote the applied equation-of-state model in the corresponding Tables and Figures.

$$AAD = \frac{1}{n}\sum_{i=1}^{n}\left|10^2 * \frac{\rho_{i,exp} - \rho_{i,EoS}}{\rho_{i,EoS}}\right| \qquad (20)$$

$$Bias = \frac{1}{n}\sum_{1=1}^{n}\left(10^2 * \frac{\rho_{i,exp} - \rho_{i,EoS}}{\rho_{i,EoS}}\right) \qquad (21)$$

$$RMA = \sqrt{\frac{1}{n}\sum_{i=1}^{n}\left(10^2 * \frac{\rho_{i,exp} - \rho_{i,EoS}}{\rho_{i,EoS}}\right)^2} \qquad (22)$$

Additionally, MaxD stands for the maximum relative deviation in the considered data set given as absolute value. For the 11 M natural gas the AAD of 0.027 from the GERG-2008 EoS was lower than the corresponding value of 0.078 from the AGA8-DC92 EoS. A similar relation was found for the RMS values, and e expectedly e GERG-2008 also produced a lower value for MaxD. However, the result for the H2-enriched natural gas was the opposite. Here, the application of AGA8-DC92 gave a lower AAD value of 0.062 compared to 0.095 for GERG-2008. Consequently, AGA8-DC92 produced lower values also for RMS and MaxD, respectively. The statistical analysis according to the Eqs. (20)-(22) was applied on some selected recently published literature data that had executed both equation-of-state models on their results for comparison.

Reference	Identifier	Covered T/K	ranges p/MPa	N	Experimental vs. GERG-2008				Experimental vs. AGA8-DC92			
					AAD	Bias	RMS	MaxD/%	AAD	Bias	RMS	MaxD/%
This work (2018)	11 M natural gas	260-350	1-20	94	0.027	−0.025	0.036	0.095	0.078	−0.078	0.081	0.127
This work (2018)	H2-enriched natural gas	260-350	1-20	99	0.095	−0.095	0.123	0.291	0.062	−0.062	0.070	0.193
Richter et al. (2014)	NG1	273-293	1.0-8.0	37	0.021	0.018	0.023	0.0375	0.010	0.001	0.013	0.0338
Richter et al. (2014)	NG2	273-293	1.0-8.0	36	0.032	0.032	0.036	0.0664	0.013	0.004	0.018	0.0509
Richter et al. (2014)	NG3	283	1.0-8.0	13	0.014	0.009	0.015	0.0256	0.027	−0.026	0.031	0.0447
Atilhan et al. (2015)	M88C1	270-340	3.5-34.5	32	0.221	−0.045	0.261	0.639	0.365	0.299	0.384	0.610
Atilhan et al. (2015)	M94C1	270-340	3.5-34.5	61	0.186	−0.144	0.215	0.516	0.094	0.039	0.112	0.361
Ahmadi et al. (2017)	natural gas	323-415	1.3-58.4	110	0.135	−0.002	0.303	2.18	0.1			

Table 7- Statistical parameters of the (p,ρ,T) data set with respect to the GERG-2008 and AGA8-DC92 EoS for the two studied natural gas mixtures including literature data for comparable mixtures.

The mixtures studied by Richter and co-workers were H2-enriched, 21-component high-calorific gases with 5 (NG1), 10 (NG2), and 30 mol-% hydrogen (NG3) originating from a pipeline. The characteristic deviation pattern found in their study looks different to our results. Data processing with GERG-2008 resulted mostly in a positive deviation that goes through a flat maximum between 4 and 6 MPa for all three mixtures. The AGA8-DC92 EoS produced more negative deviations for the respective coordinates, but the values for AAD, Bias, and RMS turned out to be smaller than the corresponding values for the GERG-2008 EoS except for NG3, i.e., the mixture with the highest hydrogen content of 30 mol-%. The mixtures studied by Atilhan et al. contained heavier alkanes but

no hydrogen [54]. The methane content of M88C1 (88 mol-%) was smaller than for M94C1 (94 mol-%) with that difference being merely compensated by higher amounts of ethane (5.8 mol-% for M88C1 and 1.9 mol-% for M94C1) and propane (3.3 mol-% for M88C1 and 1.8 mol-% for M94C1), respectively. In both mixtures, carbon dioxide (1.5 mol-%) and nitrogen (2.5 mol-%) were at approximately similar concentrations. Data analysis with the GERG-2008 EoS resulted in a sinusoid function of both positive (at $p > 25$ MPa) and negative (at $p < 25$ MPa) deviations, with no significant temperature dependence for M88C1. The corresponding diagram of M94C1, however, shows mostly negative deviations that turn into positive values not before $p > 30$ MPa. A temperature dependence clearly manifested in the largest deviation at low temperatures. Data processing of M88C1 with the AGA8-DC92 EoS gave a similar pattern but with a stronger temperature dependence than for GERG-2008; the results for M94C1 display a good coincidence with minor deviations only. An assessment of the statistical parameters given in Table 7 states a better performance of GERG-2008 on M88C1 and of AGA8- DC92 on M94C1. However, the difference between the two models remains rather small. Ultimately, Ahmadi et al. [55] investigated a rather “ordinary” natural gas mixture of 7 compounds (methane: 88 mol-%, ethane: 6.0 mol-%, propane: 2.0 mol-%, n-butane: 0.3 mol-%, isobutane: 0.2 mol-%, carbon dioxide: 2.0 mol-%, nitrogen: 1.5 mol-%). A characteristic feature of their results (the detailed plot was provided for the GERG-2008 EoS only) is that scattering and (significant) deviation starts at about pressures of 15 MPa and further increases towards lower pressure. When this area is not considered in the analysis, experimental and calculated data show good coincidence even at the highest pressures investigated. In the second experiment the validity of the code has been developed for this study is checked by comparing the calculated results for a sample natural gas with existing data in the literature. Numerous pressure and temperature points were randomly selected for this comparison. The manual validation revealed no error in the written script for this study. The Eos GERG-2008 is valid for temperatures, pressures and compositions of obtaining a very high precision of the thermodynamic properties. For some binary mixes only the reduction functions have been used. However, the GERG-2008 EoS has been extensively compared with available data and its validity range can be divided into three pressure/ temperature ranges:

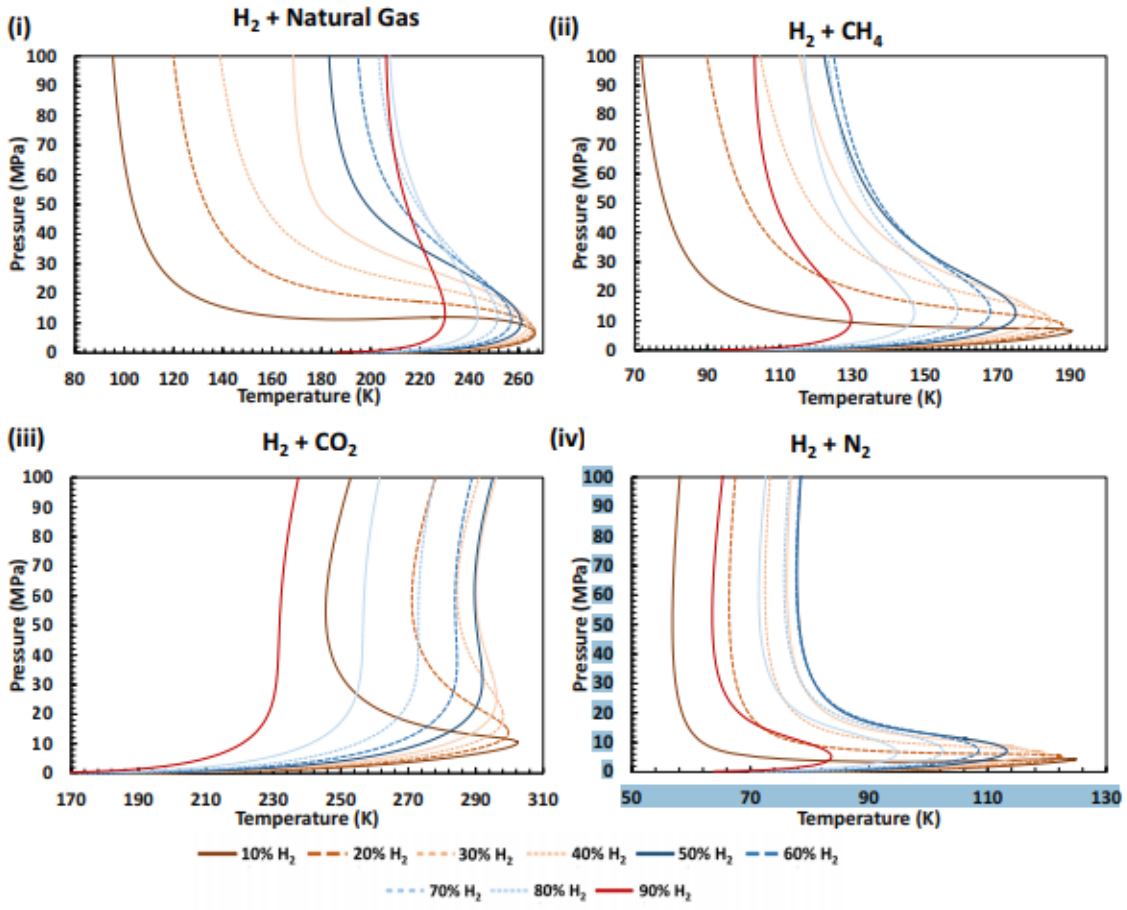

Figure 14- Modelled Vapor liquid Equilibria (VLE) diagrams using the developed tool in this study for various H2 containing mixtures with different H2 mole fractions over a wide range of pressures and temperatures.

They refer readers to an excellent book on thermodynamics and phase behavior of fluids to read more details about the behavior of mixed fluids under various pressure and temperature conditions [56].

Componenti	Mole %
CH4	83.60
C2H4	7.48
C3H8	3.92
n-C4	0.81
i-C4	0.81
n-C5	0.15
i-C5	0.14
N2	1.95
CO2	1.14

Table 8- Natural gas molar composition used in this study. The composition is based on data obtained from a typical UK North Sea natural gas [57].

• Normal range: which covers temperatures between 90K and 450K and pressures up to 35MPa (The uncertainty of calculated density is less than 0.1% over the major part of this range).

•Extended range: which covers temperatures between 60K and 700K and pressures up to 70MPa (The uncertainty of calculated density is less than 0.5% over the major part of this range).

•Extrapolated range: which covers temperatures and pressures beyond the previous range. (The uncertainty of

calculated density is less than 1% over the major part of this range up to 100MPa).

A number of studies using the same thermodynamic models have demonstrated the validity and accuracy

of GERG-2008 EoS for different mixtures such as CH4 mixtures (55,56), CO2 mixtures (57,58), natural gas (59,60) and compressed air (61).

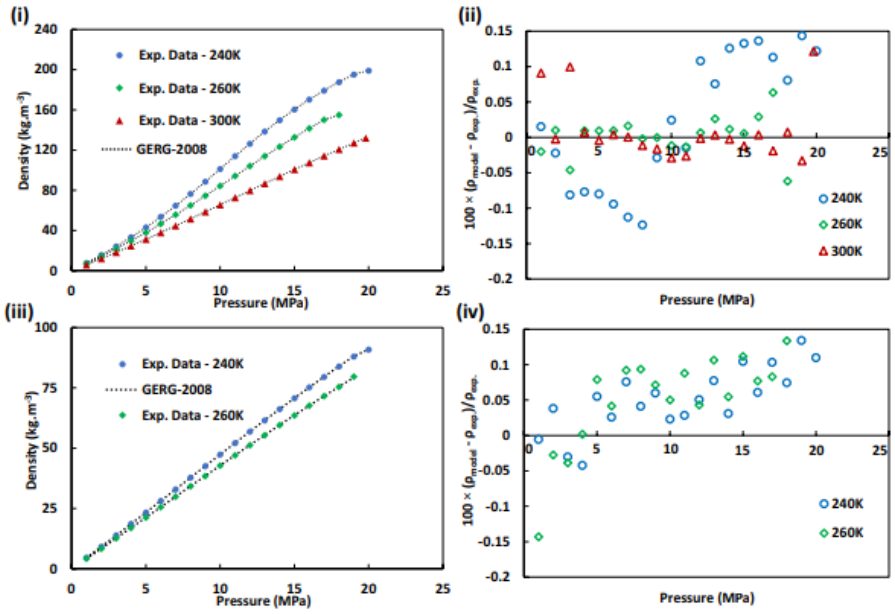

Figure 15- Thermodynamic modelling and experimental results of density of hydrogen/methane mixtures at a range of temperatures and pressures: i & ii are the results for a10%H2+90%CH4 mixture and iii & iv are the results for a 50%H2+50%CH4 mixture at different pressure and temperatures. ii and iv show the relative deviations in density values predicted by GERG-2008 equation of state, ρ_{model}, from the density from the experimental (ρ_{exp}.) data versus pressure at different temperatures. The relative expanded uncertainties in experimental density (k=2) U(ρ_{exp}) for the10%H2 + 90%CH4 mixture and the 50%H2 + 50%CH4 mixture are 0.024 ≤ U(ρ_{exp}) ≤ 0.046 and 0.024 ≤ U(ρ_{exp}) ≤ 0.034, respectively.

In the third experiment In the fourth experiment there are several applications which require accurate thermodynamic data for hydrogen rich hydrocarbons. Some of these applications are as follows:

- **Methyl Tertiary Butyl Ether (MTBE):** The need for high octane unleaded gasoline and clean air is increasing the demand for oxygen containing additives to gasoline, such as MTBE. This product reduces the carbon monoxide in the exhaust gas while enhancing the octane number of the gasoline. The process requires refrigeration in which peak cold is generated by expansion of a hydrogen rich hydrocarbon gas.
- **Ethylene Plants:** High ethylene recovery from the tail gas that is normally used as a fuel is possible by using a turboexpander. All ethylene process plants using turboexpander(s) have process gas in two phase operation. Through a cryogenic process, most of the ethylene and almost all of the heavier hydrocarbon components are liquified in one process.
- **Propylene Plants:** Many refineries are also using a similar process to fractionate propylene from the liquid feed.

- **Hydrogen Purification:** Traces of impurities such as nitrogen, carbon monoxide and methane may be separated after liquification at deep cryogenic temperatures. The preferred process design uses turboexpanders to produce the deep cryogenic temperatures.

In the fifth experiment Comparisons of calculated properties to measurements provide the basis for assessment of the accuracy and precision of the experimental data and the quality of the representation of the surface of state by the available model(s). The definitions for the statistical parameters are given below:

$$AAD = \frac{1}{n}\sum_{i=1}^{n}|\%\,\Delta X_i|,\ where\ \%\Delta X = 100\left(\frac{X_{data} - X_{calc}}{X_{data}}\right) \quad (23)$$

X is any property, n is the number of data points in the data set, and i is the index for each data point. Comparisons were made to the NIST Standard Reference Database Program REFPROP, which implements the parahydrogen equation of state of Younglove that uses the IPTS-68 temperature sale, and the upper limits in pressure and temperature are 121 MPa and 400 K. The equation of state for normal hydrogen uses the real fluid portion of the parahydrogen equation of state coupled with the ideal-gas heat capacity equation for normal hydrogen.

3 EQUATIONS OF STATE

In thermodynamics and physical chemistry, an equation of state is a constitutive law that describes the state of matter under a given set of physical conditions. It provides a mathematical relationship between two or more state variables associated with matter, such as temperature, pressure, volume or internal energy. Equations of state are useful in describing the properties of fluids (and their mixtures) and solids.

The main use of an equation of state is to determine the state parameters for gases and liquids.

Several more accurate equations of state have therefore been developed for gases and liquids. There is currently no single equation of state that accurately describes the properties of all substances under different possible conditions.

3.1 Pure H2 modelling

In the second experiment the thermo-physical properties of hydrogen mixed gases are crucial to understand and model hydrogen transportation and flow measurement processes. Termo-physical properties of hydrogen-containing gas mixtures over a wide range of pressures and temperatures are pivotal to the design and optimisation of hydrogen production units, transportation, and storage

processes. Significant effort has been made to investigate the thermodynamic properties of hydrogen-containing mixtures systematically. In addition, the phase equilibria and solubility of Hydrogen-natural gas components contained blends have been studied by researchers. While the thermodynamic properties of pure hydrogen are well established, published properties of gas mixtures in relation to geological hydrogen storage do not cover the full range of additional gasses and often do not encompass the pressures and temperatures encountered within the hydrogen storage system. They come quantify the impacts of these additional gas components, to enable the accurate simulation of hydrogen mixed with various gases, all of which are essential for the modelling of the transportation, injection, geological storage, and production of hydrogen over multiple injection/production cycles. In the fifth experiment written by R. T Jacobsen, J. W. Leachman, S. G. Penoncello, E. W. Lemmon, hydrogen undergoes changes as it is used in the production of chemicals, in oil refining, in the treatment of metals. To use hydrogen in these tasks, it must be transformed, and pressures and temperatures were required to transform it. To do this, the Younglove equation of state (equation 23) was used which made it possible to develop new models that can extend the temperature and pressure ranges.

3.2 H2-rich mixtures modelling

In the first experiment the approved ISO standard (ISO 20765-2) for the calculation of thermophysical properties of established natural gas-type mixtures is the GERG-2008 equation of state [58-59]. The addition of hydrogen will contribute further diversification to the composition of those mixtures. The performance of equation-of-state (EoS) models, such as the GERG-2008 EoS or the AGA8-DC92 EoS developed by the American Gas Association [60], must be validated using consolidated volumetric (pVT) data of high accuracy. The mixtures for this study were prepared from a 21-component high-calorific pipeline gas that was blended with hydrogen to a hydrogen content of approximately 5, 10, and 30 mol-%. Volumetric data were recorded at temperatures between 273 and 293 K and up to a maximum pressure of 8 MPa using a two-sinker densimeter. The experimental density data were compared with calculated values from both the GERG-2008 and the AGA8-DC92 EoS. For both EoS, the relative deviations in density remained below 0.05% for the 5- and 10-% mixture but raised to a value of about 0.1% for the 30-% mixture. The authors explained latter with larger errors in the composition analysis at a high hydrogen content. In another volumetric study on mixtures, Atilhan, Aparicio, Hall, and co-authors [61] have employed a (H2-free) deepwater natural gas mixture with heavy hydrocarbon content (i.e., C6þ up to n-C9 > 0.2 mol-%) that were gravimetrically prepared and traceable to the National Institute of Standards and Technology NIST [62]. Since the authors intended to explore the limits of the equation-of-state

models (both GERG2008 and AGA8-DC92), the experiments were conducted at temperatures between 270 and 340 K and up to pressures of 35 MPa using a magnetic suspension densimeter. They found density deviations larger than 0.1% especially for pressures < 10 MPa in the vicinity of the phase envelope for both models. Chapoy and co-workers determined densities and speedof-sound values of a synthetic natural gas (88 mol-% of methane) with certified composition at temperatures between 323 and 415 K and pressures up to 58 MPa. Using a highpressure and high-temperature vibrating-tube densimeter and a specially adapted in-house made acoustic cell. Additionally, an isochoric cell was employed to cover the entire operational range. In addition to GERG-2008 and AGA8-DC92 EoS, the (cubic) Peng-Robinson [63] and the Soave-BenedictWebb-Rubin [64] EoS were used to evaluate the experimental data and to calculate various derivable thermodynamic properties. The Peng-Robinson EoS featured a maximum deviation in the predicted density of about 2.8%, whereas the maximum deviation for the other models did not exceed 0.7%. This work provides new high-precision experimental (p, r, T) data for two gravimetrically prepared natural gas mixtures. Both mixtures also qualify as primary calibration standards. The first mixture resembled a conventional natural gas of 11 components and is labeled BAM-G 420 or 11 M according to the specification given in the directive PTB-A 7.63 by the Physikalisch-Technische Bundesanstalt PTB. The second mixture was a 13-component H2-enriched natural gas mixture 21984 international journal of hydrogen energy 43 (2018) 21983 e21998 with a low calorific value to facilitate support to power-to-gas applications which was proposed by the Consultative Committee for Amount of Substance: Metrology in Chemistry and Biology (CCQM) of the Bureau International des Poids et Mesures (BIPM) for the interlaboratory key comparison K 118 [65]. Density measurements were performed at temperatures between 260 and 350 K and at pressures up to 20 MPa using a single sinker densimeter with magnetic suspension coupling. 94 data points were recorded and 99 for the H2- enriched gas mixture, respectively, in an isothermal operational mode at 260, 275, 300, 325, and 350 K. The data were compared with the corresponding densities calculated from GERG-2008 and AGA8-DC92 EoS, via REFPROP, and can thus give an assessment for the performance of these models on novel compositions of energy gases. In the fourth experiment there are several predictions methods for properties of mixtures from low molecular weight systems to complex heavy hydrocarbon mixtures. The most common equations are Peng-Robinson (PR), Soave-Redlich-Kwong (SRK), and Benedict-Webb-Rubin-Starling (BWRS). [66,67,68] Newton was the first to suggest that hydrogen could be evaluated with other gases by replacing their true critical constants with the effective critical constants. [69] His correlation showed an improvement in PVT data at room temperature but demonstrated somewhat poorer results at lower temperature

conditions. Newton's correlation has been modified over the years by using effective critical constants instead of true critical constants. For hydrogen rich hydrocarbons there are additional equations of state such as: Chao-Seader, Grayson-Streed, and Zudkevitch-Joffe, since hydrogen is used in the development of their respective models. (70,71,72) The PR and SRK equations of state uses binary interaction parameters. The ZJ equation is a modified model of RK for the better prediction of the systems containing hydrogen. The CS and GS methods are semiempirical with GS correlation being an extension of CS equations with specific emphasis on hydrogen. Mohsen-Nia et al. developed a simple and accurate cubic equation of state for the prediction of thermodynamic properties and phase behavior of sour natural gas and liquid mixtures containing hydrogen. [73] The latter equations of state is designed specifically to predict thermodynamic properties and phase equilibria of liquid and vapors which consist of hydrogen, methane and light hydrocarbons. Because of quantum effects, hydrogen and helium do not follow the simple law of corresponding states and therefore, do not fit the generalized correlations such as standard equations of state. A new simple two-constant cubic equations of state for hydrocarbons, hydrocarbon mixtures, and other non-associating fluids has been introduced by Mohsen-Nia et al. [73] This equation of state model is based on the statistical mechanical information available for the repulsive thermodynamic functions and the phenomenological knowledge of the attractive potential tail contributions to the thermodynamic properties. This new two-constant parameter cubic equation is as follows:

$$Z = \frac{(v+1.3191b)}{(v-b)} - \frac{a}{\left[RT^{\frac{3}{2}}(v+b)\right]} \qquad (24)$$

Equation (1) is cubic in terms of volume and contains only two adjustable parameters. By applying the critical point constraints on the above equation, parameters a and b are determined to be:

$$a = 0.486989\, R^2 T_c^{\frac{3}{2}} / P_c \qquad b = 0.064662\, RT_c/P_c \qquad (25)$$

The critical compressibility factor based on these equations of state is calculated to be:

$$Z_C = \frac{1}{3} \qquad (26)$$

The latter calculation is the same as the Redlich-Kwong (RK) equations of state. It has been shown, however, that these equations of state are more accurate than the Redlich-Kwong equation, which

had been considered to be the best two-constant-parameter cubic equation of state for quite some time. (32) For multi-component mixtures this equation of state takes the following form:

$$Zm = (v + 1{,}3191 b_{Rm})/\,(v - b_{Am}) \; - \; a_m/[RT^{\frac{3}{2}}(v + b_{Am}) \quad (27)$$

where they use the following mixing rule for am, bAm and bRm:

$$a_m = \sum_i \sum_j x_i x_j a_{ij} \quad (28)$$

$$b_{Rm} = \left(\frac{3}{4}\right) \sum_i \sum_j x_i \, x_j b_{ij} \; + \left(\frac{1}{4}\right) \sum_i x_i b_{ij} \quad (29)$$

$$b_{Am} = \; \sum_i x_i b_{ii} \quad (30)$$

Subscript R in bRm stands for the repulsive mixing rule and subscript A in bAm stands for the attractive mixing rule of b. For reasons mentioned elsewhere, the mixing rule for parameter b when it appears in the repulsive (positive) term of the equation of state (bRm) will be different from that of the attractive (negative) term (bAm). For unlike interaction parameters au and (bAm), the following combining rules are used.

$$b_{ij} = \frac{\left(b_{ii}^{\frac{1}{3}} + b_{jj}^{\frac{1}{3}}\right)^3}{8} \quad (31)$$

$$a_{ij} = \left(1 - \; k_{ij}\right) \left(a_{ii} a_{jj}\right)^{1/2} \qquad (32)$$

Parameter k_{ij} is defined as the coupling parameter which can be determined using some mixture data. The theoretical foundations for the choice of the above mixing and combining rules are also discussed elsewhere. The above cubic equations of state has been used for calculating the thermodynamic properties of hydrocarbons and other non-associating fluids and fluid mixtures, and it has been shown that this two-constant cubic equation of state and its mixture version are far superior to the RK equation of state which is also a two-constant cubic equation. However, the better accuracies achieved by this simple cubic equation of state is still not sufficient to allow it to be used for engineering design calculations of turboexpanders. In order to improve the accuracy of

the present equation of state to the level that it could be used for engineering design calculations, it is necessary to make parameters a and b temperature-dependent similar to the many modifications of the van der Waals and RK equations of state. For this purpose, they replace parameters "a" and 'b" with the following temperature-dependent expressions.

$$a = a_c\,\alpha\,(T_r) \qquad b = b_c\beta\,(T_r) \qquad (33)$$

Where

$$a_c = 0{,}486989\,R^2T_e^{5/2}/\;P_{e'} \qquad b_c = 0{,}064662\,RT_c/P_c \quad (34)$$

The dimensionless temperature-dependent parameters α(Tr) and δ(Tr), while different from each other, reduce to unity at the critical point:

$$\alpha\,(T_r = 1) = \;\beta\,(T_r = 1) = 1 \qquad (35)$$

There have been a variety of empirical functional forms for α and β reported in the literature. However, in line with the variational and perturbation molecular theories of fluids Equation (31), the following polynomial expression for β(T_r) may be used:

$$\beta(T_r)^{1/3} = \frac{\left[1+\frac{\beta_1}{T_r}+\frac{\beta_2}{T_r^2}+..\right]}{[1+\beta_1+\beta_2+\cdots]} \qquad (36)$$

Then for simplicity, and as a first approximation, the following form for β(T_r) is used.

$$\beta(T_r) = \frac{\left(1+\frac{\beta}{T_r}\right)^3}{(1+\beta_1)^3} \qquad (37)$$

where β1 is a constant. Equation (37) satisfies the basic theoretical conditions for β(Tr) at the critical point, i.e.: β(Tr)→1 at Tr→1. This functional form will remain finite and positive for all possible temperature ranges. For symmetry and simplicity, the same functional form for parameter α(Tr), maybe used i.e.

$$\alpha(T_r) = \frac{\left(1+\frac{\alpha_1}{T_r}\right)^3}{(1+\alpha_1)^3} \quad (38)$$

Where α1 is a constant. Equation (38) also satisfies the basic theoretical conditions for α(Tr) at the critical point, i.e.: α(Tr)→1 at Tr→1. It can also be inferred from the form of these equations of state that as temperature tends to infinity, the attractive term -a/[RT3/2(v+b)], must also approach zero. The form of α(Tr) considered in this work is conducive to this requirement. The constants α1 and β1 have been determined for the components of hydrogen and sour natural gas mixtures and of hydrogen gas-condensate mixtures and are reported in Table 9. These constants were found by minimization of the vapor pressures and saturation liquid densities. For ease of calculations, parameters al and α1 and β1 are correlated for the major components of natural gas (see Table 9) to their eccentric factor in the following forms:

$$\alpha_1 = 0.036139 - 0{,}14167\omega;\ \beta_1 = 0.0634 - 0.18769\omega\ for - 0.22 \leq \omega \leq 0.18 \quad (39)$$

These correlations are for co in the range of -0.22 ≤ ω ≤ 0 .18 and they do not hold very well for parameters of components of natural gas which are in minute quantities (C_4 - C_7^+). Because of very small concentrations of these components in natural gas streams, however, application of the above correlation Equation (38) for these components will not cause any appreciable error in the computation of thermodynamic properties for hydrogen and natural gas mixtures. Formulation of equations of state of hydrocarbon mixtures containing appreciable amounts of heavier hydrocarbons requires application of the continuous thermodynamics and C_7^+ fraction characterization techniques Equations (33), (34), and (35).

One of the requirements of equations of state for industrial applications is their analytic representation of thermodynamic functions. Such properties of fluids (like entropy, enthalpy, and fugacity) are of direct interest in energy balance and phase behavior calculations in industrial practice. The analytic expressions of these functions are as follows:

SUBSTANCE	α1 major components	β1 of natural gas
H2	-0.07099	0.12307
N2	-0.02474	0.06393
co	-0.02281	0.06066
CO2	-0.00580	0.01456
H2S	-0.02351	0.04207
CH4	-0.03662	0.05957
C2H4	-0.02898	0.03865
C2H6	-0.02133	0.04504
C3H6	-0.00841	0.04624
C3H8	-0.01457	0.03657
Components of natural gas		
n-C4H10	-0.00663	0.03613
i-C4H10	-0.01373	0.02852
n-C5H12	-0.00878	0.02251
n-C6H14	-0.00761	0.01258
n-C7H16	-0.00425	0.01342

Table 9

4 CONCLUSION

In this thesis work, an investigation on thermodynamic properties of hydrogen was presented. The work included several research articles published in international journals with regards to hydrogen and hydrogen-rich mixtures. Experimental setup and theoretical investigations have been included in order to assess the accuracy of the most commonly used models and EoS. In the first experiment analyzed, new high-precision experimental (p, r, T) data for two multicomponent natural gas mixtures were recorded. The gas mixtures for the study mimic real natural gas mixtures, one being a conventional 11-component gas, the other a 13-component H2-enriched mixture proposed by CCQM. The experiments were done using a single sinker densimeter with magnetic suspension coupling in a temperature range between 260 and 350 K and up to pressures of 20 MPa. A comparison of the performance of both equation-of-state models shows that GERG-2008 performs better on 11 M than AGA8-DC92. The results for the H2-enriched gas mixtures are different. The deviations of experimental data from the GERG-2008 EoS are not within the 0.1% margin at high pressures, this pressure limit being lower for lower temperatures (17 MPa for 350 K, and only 9 MPa for 260 K). In the second experiment have been published density data of hydrogen/methane blends at a range of pressure and temperature conditions to statistically analyse and assess the reliability and accuracy of the attained modelling data from the GERG-2008 EoS. In the third experiment it has been noted that for predicting the properties of hydrogen for the whole range (saturated and supercritical conditions) the RKMC EoS is accurate and robust. Therefore, based on the data analyzed, the RKMC EoS is recommended for most applications connected with hydrogen. For predicting hydrogen properties at temperatures greater than 200 K, almost all EoSs can be used with comparable accuracy. In the fourth experiment, several equations of state have been analyzed by the authors and evaluated using available field performance data, however, the study was limited to the gas dynamic behaviour of turboexpander using hydrogen-rich natural gas as a process fluid. Finally, since several differences have been highlighted between the experiments analyzed, it is not possible to define the most correct method to use as each method is applied to a particular situation and with conditions. In general, it is suggested to analyze the fit-for-purpose solutions based on the situation and then apply one of the methods described in this work.

5 Bibliography

[1] Wagner W, Kleinrahm R. Densimeters for very accurate density measurements of fluids over large ranges of temperature, pressure, and density. Metrologia 2004;41: S24e39. https://doi.org/10.1088/0026-1394/41/2/S03.

[2] McLinden MO, Kleinrahm R, Wagner W. Force transmission errors in magnetic suspension densimeters. Int J Thermophys 2007; 28:429e48. https://doi.org/10.1007/s10765- 007-0176-0.

[3] Richter M, Kleinrahm R. Influence of adsorption and desorption on accurate density measurements of gas mixtures. J Chem Thermodyn 2014; 74:58e66. https://doi.org/ 10.1016/j.jct.2014.03.020.

[4] Hernandez-Gomez R, Tuma D, Segovia JJ, Chamorro CR. Experimental determination of (p, r, T) data for binary mixtures of methane and helium. J Chem Thermodyn 2016; 96:1e11. https://doi.org/10.1016/j.jct.2015.12.006.

[5] Hernandez-Gomez R, Tuma D, Perez E, Chamorro CR. Accurate experimental (p, r, and T) data for the introduction of hydrogen into the natural gas grid (II): thermodynamic characterization of the methaneehydrogen binary system international journal of hydrogen energy 43 (2018) 21983 e21998 21997from 240 to 350 K and pressures up to 20 MPa. J Chem Eng Data 2018; 63:1613e30. https://doi.org/10.1021/acs.jced.

[6] Kunz O, Wagner W. The GERG-2008 wide-range equation of state for natural gases and other mixtures: an expansion of GERG-2004. J Chem Eng Data 2012; 57:3032e91. https:// doi.org/10.1021/je300655b.

[7] Kunz, O. & Wagner, W. Te GERG-2008 wide-range equation of state for natural gases and other mixtures: an expansion of GERG-2004. J. Chem. Eng. data 57, 3032–3091 (2012).

[8] Klimeck, R. Entwicklung einer Fundamentalgleichung für Erdgase für das Gas-und Flüssigkeitsgebiet sowie das Phasengleichgewicht. (2000).

[9] Hassanpouryouzband, A., Joonaki, E., Edlmann, K., Heinemann, N. & Yang, J. Termodynamic and Transport Properties of Hydrogen Containing Streams: Data sets. fgshare https://doi.org/10.6084/m9.fgshare.12063297 (2020).

[10] Huber, M. L. Models for Viscosity, Termal Conductivity, and Surface Tension of Selected Pure Fluids as Implemented in REFPROP v10. 0. (2018).

[11] Chung, T. H., Ajlan, M., Lee, L. L. & Starling, K. E. Generalized multiparameter correlation for nonpolar and polar fuid transport properties. Ind. Eng. Chem. Res. 27, 671–679 (1988).

[12] Lohrenz, J., Bray, B. G. & Clark, C. R. Calculating Viscosities of Reservoir Fluids from Teir Compositions. J. Pet. Technol. 16, 1171–1176 (1964).

[13] Ely, J. F. & Hanley, H. J. M. Prediction of transport properties. 2. Termal conductivity of pure fuids and mixtures. Ind. Eng. Chem. Fundam. 22, 90–97 (1983).

[14] Dagaut P, Dayma G. Hydrogen-enriched natural gas blend oxidation under high pressure conditions: experimental and detailed chemical kinetic modelling. Int J Hydrogen Energy 2006; 31:505–15.

[15] Otsuka K, Shigeta Y, Takenaka S. Production of hydrogen from gasoline range alkanes with reduced CO2 emission. Int J Hydrogen Energy 2002; 27:11–8.

[16] Vagia ECh, Lemonidou AA. Thermodynamic analysis of hydrogen production via steam reforming of selected components of aqueous bio-oil fraction. Int J Hydrogen Energy 2007; 32:212–23.

[17] Garcia EY, Laborde MA. Hydrogen production by the steam reforming of ethanol: thermodynamic analysis. Int J Hydrogen Energy 1991; 6:307–12.

[18] Wang H, Wang X, Li M, Li S, Wang S, Ma X. Thermodynamic analysis of hydrogen production from glycerol auto thermal reforming. Int J Hydrogen Energy 2009; 34:5683–90.

[19] Sadus RJ. Influence of quantum effects on the high-pressure phase behavior of binary mixtures containing hydrogen. J Phys Chem 1992; 96:3855–60.

[20] Flourusse LJ, Peters CJ, Pa`mies JC, Vega LF, Meijer H. Solubility of hydrogen in heavy n-alkanes: experiments and SAFT modeling. AIChE J 2003; 49:3260–9.

[21] Boublı´k T. The BACK equation of state for hydrogen and related compounds. Fluid Phase Equilib 2005; 240:96–100.

[22] Ibrahimoglu B, Veziroglu TN, Huseynov A. Study of thermodynamic parameters of hydrogen gas by grapho analytic method. Int J Hydrogen Energy 2005; 30:515–9.

[23] Chen H, Zheng J, Xu P, Li L, Bie H. Study on real-gas equations of high-pressure hydrogen. Int J Hydrogen Energy, doi:10. 1016/j.ijhydene.2009.08.029.

[24] Ferrando N, Ungerer P. Hydrogen/hydrocarbon phase equilibrium modeling with a cubic equation of state and a Monte Carlo method. Fluid Phase Equilib 2007;254: 211–23.

[25] Moysan JM, Huron MJ, Paradowski H, Vidal J. Prediction of the solubility of hydrogen in hydrocarbon solvents through cubic equations of state. Chem Eng Sci 1983; 38:1085–92.

[26] Huang H, Sandler SI, Orbey H. Vapor–liquid equilibria of some hydrogen þ hydrocarbon systems with the Wong– Sandler mixing rule. Fluid Phase Equilib 1994; 96:143–53.

[27] Yang JC. A thermodynamic analysis of refueling of a hydrogen tank. Int J Hydrogen Energy 2009; 34:6712–21. [15] Hadj-Kali MK, Gerbaud V, Borgard J-M, Baudouin O, Floquet P, Joulia X, et al. HIx system thermodynamic model 3810 international journal of hydrogen energy 35 (2010) 3802–3811for hydrogen production by the sulfur–iodine cycle. Int J Hydrogen Energy 2009; 34:1696–709.

[28] Peng DY, Robinson DB. A new two-constant equation of state. Ind Eng Chem Fundam 1976; 15:59–64.

[29] Paricaud P, Tazi L, Borgard LM. Modeling the phase equilibria of the HIx mixture using the SAFT-VR equation of state: binary systems. Int J Hydrogen Energy, doi:10.1016/j. ijhydene.2009.11.025.

[30] Gil Villegas A, Galindo A, Whitehead PJ, Mills SJ, Jackson G, Burgess AN. Statistical associating fluid theory for chain molecules with attractive potentials of variable range. J Chem Phys 1997; 166:4168–86.

[31] Mohamed K, Paraschivoiu M. Real gas simulation of hydrogen release from a high-pressure chamber. Int J Hydrogen Energy 2005; 30:903–12.

[32] Beattie JA, Bridgeman BC. A new equation of state for fluids. I. Application to gaseous ethylether and carbon dioxide. J Am Chem Soc 1927; 49:1665–7.

[33] Schouten JA, Janssen-Van Rosmalen R, Michels JPJ. Condensation in gas transmission pipelines. Phase behavior of mixtures of hydrogen with natural gas. Int J Hydrogen Energy 2005; 30:661–8.

[34] Uilhoorn FE. Dynamic behavior of non-isothermal compressible natural gases mixed with hydrogen in pipelines. Int J Hydrogen Energy 2009; 34:6722–9.

[35] Holderbaum T, Gmehling J. PSRK: a group contribution equation of state based on UNIFAC. Fluid Phase Equilib 1991; 70:251–65.

[36] Zhou L, Zhou Y. Determination of compressibility factor and fugacity coefficient of hydrogen in studies of adsorptive storage. Int J Hydrogen Energy 2001; 26:597–601.

[37] Soave G. Equilibrium constants from a modified Redlich– Kwong equation of state. Chem Eng Sci 1972; 27:1197–203. [26] Benedict M, Webb GB, Rubin LC. An empirical equation for thermodynamic properties of light hydrocarbons and their mixtures, methane, ethane, propane and n-butane. J Chem Phys 1940; 8:334–45.

[38] Aktasx S, Karakaya M, Avci AK. Thermodynamic analysis of steam assisted conversions of bio-oil components to synthesis gas. Int J Hydrogen Energy 2009; 34:1752–9.

[39] Zheng J, Ye J, Yang J, Tang P, Zhao L, Kern M. An optimized control method for a high utilization ratio and fast filling speed in hydrogen refueling station. Int J Hydrogen Energy, doi: 10.1016/j.ijhydene.2009.07.001.

[40] Yang JC, Huber ML. Analysis of thermodynamic processes involving hydrogen. Int J Hydrogen Energy 2008; 33:4413–8.

[41] NIST Chemistry Webbook. Available via the internet at: http://webbook.nist.gov/chemistry/.

[42] Nasrifar Kh, Bolland O, Moshfeghian M. Predicting natural gas dew points from 15 equations of state. Energy & Fuels 2005; 19:561–72.

[43] Abdollah-Demneh F, Moosavian MA, Montazer-Rahmati MM, Omidkhah MR, Bahmaniar H. Comparison of the prediction power of 23 generalized equations of state: part 1. Saturated thermodynamic properties of 102 pure substances. Fluid Phase Equilib 2010; 288:67–82.

[44] Wei YS, Sadus RJ. Equations of state for the calculation of fluid-phase equilibria. AIChE J 2000; 46:169–96.

[45] Valderrama JO. The state of the cubic equations of state. Ind Eng Chem Res 2003; 42:1603–18.

[46] Eubank PT, Wang X. Saturation properties from equations of state. Ind Eng Chem Res 2003; 42:3838–44

[47] Prausnitz JM, Tavares FW. Thermodynamics of fluid-phase equilibria for standard chemical engineering operations. AIChE J 2004; 50:739–61.

[48] Patel NC, Teja AS. A new equation of state for fluids and fluid mixtures. Chem Eng Sci 1982; 37:463–73.

[49] Nasrifar Kh, Bolland O. Prediction of thermodynamic properties of natural gas mixtures using 10 equations of state including a new two-constant equation of state. J Pet Sci Eng 2006; 51:253–66.

[50] van der Waals JD. Molekulartheorie eines Korpers der ans zwei ver-schiedene Stoffen bestecht. Z Phys Chem 1890;5: 133–73.

[51] Salim PH, Trebble MA. A modified Trebble–Bishnoi equation of state: thermodynamic consistency revisited. Fluid Phase Equilib 1991; 65:59–71.

[52] Hernandez-Gomez R, Tuma D, Gomez-Hernandez A, Chamorro CR. Accurate experimental (p, r, T) data for the introduction of hydrogen into the natural gas grid: thermodynamic characterization of the nitrogen hydrogen binary system from 240 to 350 K and pressures up to 20 MPa. J Chem Eng Data 2017; 62:4310e26. https://doi.org/10.1021/ acs. jced.7b00694.

[53] Lemmon EW, Huber ML, McLinden MO. NIST standard reference database 23: reference fluid thermodynamic and transport properties-REFPROP, version 9.1. Gaithersburg MD: National Institute of Standards and Technology, Standard Reference Data Program; 2013.

[54] Atilhan M, Aparicio S, Ejaz S, Zhou J, Al-Marri M, Holste JJ, et al. Thermodynamic characterization of deepwater natural gas mixtures with heavy hydrocarbon content at high pressures. J Chem Thermodyn 2015; 82:134e42. https:// doi.org/10.1016/j.jct.2012.04.008.

[55] Ahmadi P, Chapoy A, Tohidi B. Density, speed of sound and derived thermodynamic properties of a synthetic natural gas. J Nat Gas Sci Eng 2017; 40:249e66. https://doi.org/10.1016/ j. jngse.2017.02.009.

[56] Danesh, A. PVT and phase behaviour of petroleum reservoir fuids. (Elsevier, 1998).

[57] NLOG. Gas Properties, https://www.nlog.nl/en/gas-properties (2006)

[58] Kunz O, Wagner W. The GERG-2008 wide-range equation of state for natural gases and other mixtures: an expansion of GERG-2004. J Chem Eng Data 2012;57:3032e91. https:// doi.org/10.1021/je300655b

[59] ISO 20765-2. Natural gas e calculation of thermodynamic properties e Part 2: single-phase properties (gas, liquid, and dense fluid) for extended ranges of application. Geneva: International Organization for Standardization; 2015.

[60] Starling KE, Savidge JL. Compressibility factors of natural gas and other related hydrocarbon gases e AGA Transmission Measurement Committee Report No. 8. 2nd ed. Washington DC: American Gas Association; 1992.

[61] Atilhan M, Aparicio S, Ejaz S, Zhou J, Al-Marri M, Holste JJ, et al. Thermodynamic characterization of deepwater natural gas mixtures with heavy hydrocarbon content at high pressures. J Chem Thermodyn 2015; 82:134e42. https:// doi.org/10.1016/j.jct.2012.04.008.

[62] Ahmadi P, Chapoy A, Tohidi B. Density, speed of sound and derived thermodynamic properties of a synthetic natural gas. J Nat Gas Sci Eng 2017; 40:249e66. https://doi.org/10.1016/ j. jngse.2017.02.009.

[63] Peng D-Y, Robinson DB. A new two-constant equation of state. Ind Eng Chem Fund 1976; 15:59e64. https://doi.org/ 10.1021/i160057a011.

[64] Soave GS. An effective modification of the Benedict-WebbRubin equation of state. Fluid Phase Equil 1999; 164:157e72. https://doi.org/10.1016/S0378-3812(99)00252-6.

[65] CCQM-K 118 Natural Gas; technical protocol V4.0d, CCQM working group on gas analysis. Sevres, France: Bureau International des Poids et Mesures BIPM; 2017.

[66] Peng, D. Y. and Robinson, D. B., "A Two Constant Equation of State", I.E.C. Fundamentals, 15, pp. 59-64 1976.

[67] Soave, G., Chem Engr. Sci., 27, No. 6, p. 1197, 1972

[68] Benedict, Webb, and Rubin, Chem. Engr. Prog. p. 47,419, 1951.

[69] Newton, R. H. ibid, 27, 302, 1935.

[70] Chao, K D. and Seader, J. D., AI.Ch.E Journal, pp. 598- 605, December 1961.

[71] Grayson, H. G. and Streed, G. W., 'Vapour-Liquid Equilibria for High Temperature, High Pressure Systems", 6th World Petroleum Congress, West Germany, June 1963.

[72] Zudkevitch, D. Joffe, J. "Correlation and Prediction of Vapor-Liquid Equilibria with the Redlich-Kwong Equation of State", AIChE Journal, Volume 16, No. 1, p. 112-119, January 1970.

[73] Mohsen-Nia, M., Moddaress, H., Mansoori, G. A, 1993. A Simple Cubic Equation of State for Hydrocarbons and other Compounds. SPE Paper #26667, Proceedings of the 1993 Anuual Technical Conference and Exhibition of the Society of Petroleum Engineers, Houston, Texas, 1993.